Role of *RanBPM* in *Drosophila* fat body for the remote control of insulin secretion and feeding behavior

Swati Agnihotri

(MSc. Thesis)

Abstract

RanBPM (Ran-Binding Protein in the Microtubule Organizing Center) is an evolutionarily conserved protein presumed to function as a scaffold in various signal transduction pathways. Null mutations in the *Drosophila RanBPM* gene cause a pleiotropic effect as seen by the late larval lethality, impaired growth, reduced CNS proliferation and disruption in feeding and response to light behaviours (Scantelbury et al., 2010). We report that *RanBPM* mutants display impaired expression and secretion of one of the major *Drosophila* insulin like peptides, DILP2. Consistent with these findings *RanBPM* mutants showed reduced membrane localization of the Phosphatidylinositol (3,4,5)-trisphosphate (PIP3) reporter TGPH (GFP-pleckstrin homology domain (PH) fusion regulated by the Tubulin promoter) and reduced activation of the serine threonine kinase AKT, both read outs of insulin signalling (InS). Ubiquitous overexpression of *DILP2* partially rescued the reduced larval growth, CNS proliferation and feeding phenotypes caused by *RanBPM* mutations. Over expression of DILP6 in the glia rescued the reduced CNS proliferation but not the reduced larval growth and feeding behaviour phenotypes. Targeted expression of *RanBPM* in the fat body suppressed all *RanBPM* mutant phenotypes except for lethality. In *Drosophila*, the fat body acts a nutritional sensor involved in coordinating neuroblast proliferation by a TOR- dependent mechanism. Our results present evidence for the role of AKT in the fat body of the *RanBPM* mutants for the regulation of CNS proliferation, DILP2 secretion, overall growth and feeding

behaviour. Furthermore, my results also suggest potential roles for *TOR* and *S6K* in the fat body for the regulation of *RanBPM* mutant phenotypes.

Acknowledgements

First, I would like to thank my supervisor, Dr. Ana Campos for providing me with the opportunity to complete my Master's program in her lab and for all her support in the recent years. I will be forever grateful for the guidance and the encouragement you provided. I will cherish our conversations and laughs for years ahead. Ana, thank you for being a great supervisor and a mentor. Thank you to Dr. Roger Jacobs and Dr. André Bédard for their insightful inputs towards my research. Special thanks to Xiao Li for making every impediment seem manageable in the lab. Words cannot justify my appreciation for the help you have been.

My overall research experience working in the fly lab has been gratifying thanks to the current and past members. Lab meetings, research discussions and stories we had shared were all memorable. I am glad to have had the chance to work with you all. To the members of Dr. Jacobs, Dr. Bedard and Dr. O'Donnell's lab, thanks for making fly work in the lab more entertaining through our stimulating discussions about fly genetics. Greatly appreciate your insights towards my research. Thanks to my friends, for encouragement during times of stress and for the great times we have spent together. My graduate experience would not have been the same without all of you.

Finally, I would like to thank my family for believing in me every step of the way. Thanks to my parents for being my guiding light and for supporting me. Thanks to my loving grandparents for their prayers and blessings.

Contributions

My thesis is a draft for a manuscript that is in the process of revision. My results will contribute to the experiments required for the completion of this manuscript. Experiments for this manuscript were designed and conceived by Dr. Ana Campos. In addition to my data, experiments performed by Xiao Li Zhao and by Dr. André Bédard comprise this manuscript. Therefore I would like to acknowledge Xiao Li's experiments highlighted in figures 3, 4, 5, 6A, 6B, 7A, 7B, 7C, section of 7D and in additional files. Western blot depicted in panel 5C was a contribution to the manuscript by Dr. Bédard. Thanks to Xiao Li and Dr. Bédard for their contributions.

Table of Contents

Abstract 2
Acknowledgements 4
Contributions 5
Table of Contents 6
List of Illustrations 8
List of Abbreviations 9

Chapter 1: Introduction

1.1 *Ran Bonding Protein in the Microtubule Organizing Center (RanBPM)* 12
1.2 *Drosophila RanBPM* 13
1.3 *Drosophila* fat body organ 14
1.4 Insulin and Target of Rapamycin (TOR) signaling 14
1.5 Remote control of insulin secretion by the fat body 17
1.6 Thesis Objectives 18

Chapter 2: Materials and Methods

2.1 *Drosophila* strains and culture 20
2.2 Feeding behaviour assay 21
2.3 Statistical Analyses 21
2.4 Immunohistochemistry and imaging 22
2.5 Western blotting analysis 23
2.6 Lysotracker staining and imaging 23
2.7 Data organization for figures 24

Chapter 3: Results

3.1 Targeted expression of *RanBPM* in neurosecretory cells rescues the disruption in feeding behaviour, reduced growth and lethality of *RanBPM* mutants 26
3.2 *RanBPM* gene function is required for proper insulin gene expression and secretion 27
3.3 *RanBPM* mutants display reduced peripheral insulin signalling 30
3.4 Forced expression of *DILPs* suppresses the feeding, size and CNS proliferation phenotypes of *RanBPM* mutants 31
3.5 Targeted expression of *RanBPM* in the fat body partially rescues most of the *RanBPM* mutant phenotypes 33
3.6 Overexpression of AKT in the fat body partially rescues *RanBPM* 35

mutant phenotypes
3.7 Up-regulation of Target of Rapamycin (TOR) or S6K in the fat body of *RanBPM* mutants partially rescues the CNS proliferation phenotype of *RanBPM* mutants 40
3.8 Autophagy in *RanBPM* mutants 41
3.9 Up-regulation of insulin signaling in the fat body 43
Chapter 4: Discussion
4.1 *Impaired insulin signaling in RanBPM mutants* 47
4.2 *Expression of RanBPM in the fat body* 48
4.3 *Ins/TOR signaling in the fat body of RanBPM mutants* 49
4.4 Conclusions 53

List of Illustrations

Figure 1.	Ins/TOR signalling.	55
Figure 2.	Schematic representation of the proposed model for *RanBPM* function.	56
Figure 3.	Targeted expression of *RanBPM* in neurosecretory cells is sufficient to rescue the feeding phenotype of *RanBPM* mutants	58
Figure 4.	Impact of *RanBPM* mutations on subsets of neurosecretory cells.	60
Figure 5.	*RanBPM* mutant phenotypes consistent with disrupted systemic insulin signaling.	62
Figure 6.	Ubiquitous expression of *DILP2* partially restores *RanBPM* mutant phenotype	64
Figure 7.	Targeted expression in the fat body rescues *RanBPM* mutant phenotype.	66
Figure 8.	Up- regulation of *AKT* in the fat body partially rescues *RanBPM* mutant phenotypes	69
Figure 9.	Targeted expression of *AKT(myr*) in the fat body of *RanBPM* mutants.	71
Figure 10.	Expression of *InR* in the fat body of *RanBPM* mutants.	72
Figure 11.	Targeted Expression of *TOR* in the fat body partially rescues the CNS proliferation of *RanBPM* mutants.	74
Figure 12.	Over expression of *S6K* in the fat body partially rescues the CNS proliferation and the size of *RanBPM* mutants.	76
Figure 13.	Targeted expression of dILPs in DIMM- positive peptidergic neurons in RanBPM mutants.	78
Figure 14.	Examining autophagy in $RanBPM^{K05201}$ mutants using LysoTracker probe.	80
Figure 15.	Measuring the size of lipid droplets in $RanBPM^{K05201}$ mutants under fed and nutrient deprived conditions.	82
Figure16.	Measure of food intake by modulating insulin signaling in the fat body.	84

List of Abbreviations

4E-BP	4E binding protein
AKH	adipokinetic hormone
AKT/PKB	protein kinase B
ALK	anaplastic lymphoma kinase
ALS	acid labile subunite
ATG	autophagy
BDNF	brain derived neurotrophic factor
CA	constitutively active
CNS	central nervous system
CTLH	C-terminal to LisH motif
dILP	*Drosophila* Insulin-like peptide
Dimm	dimmed
DN	dominant negative
FDS	fat body- derived signal
FMRP	fragile mental retardation protein
GFP	green fluorescent protein
IgG	immunoglobulin G
Imp-L2	ecdysone-inducible gene L2
InR/IGFR	insulin receptor/insulin growth factor receptor
InS	insulin signaling
IRS	insulin receptor substrate
Jeb	jelly belly
LisH	lissencephaly type-1-like homology
Lsp2	larval serum protein 2
MAPK	mitogen-activated protein kinase
MB	mushroom body
mNSC or IPC	medial neurosecretory cells or insulin producing cells
Myr	myristoylated
NB	neuroblast
NLaz	neural lazarillo
PDK	phosphoinositide dependent kinase
PH	pleckstrin homology
Phospho-H3	phosphorylated Histone H3
PI3K	phosphatidylinositol-3-Kinase
PIP2and PIP3	phosphatidylinositol-4,5-P2 and phosphatidylinositol-3,4,5-P3

Ppl	pumpless
PTEN	phosphatase and tensin homolog
RanBPM	ran binding protein in the microtubule organizing center
RHEB	RAS homologue enriched in brain
S6K	ribosomal S6 kinase
Sb	stubble
SDS	sodium dodecyl sulfate
Slif	slimfast
SPRY	spore lysis ryanodine
Tb	tubby
TOR	target of rapamycin
TORC1/2	TOR complex1 and 2
TrK	tropomyosin-related kinase
TSC1/2	tumour suppressor complex 1 and 2
UAS	upstream activating sequence
Upd2	unpaired 2
WT	wild type

Chapter 1: Introduction

Introduction

1.1 *Ran Binding Protein in the Microtubule Organizing Center (RanBPM)*

RanBPM was first identified in a yeast two hybrid screen using Ran as bait however a function in Ran- related processes have not been reported to date (Yokoyama et al., 1995; Nishitani et al., 2001; reviewed by Murrin and Talbot, 2007). In vertebrates, *RanBPM* polypeptide is comprised of multiple conserved domains involved in protein – protein interaction. Conserved domains of *RanBPM* are proline rich domain, spore lysis A and ryanodine receptor domain (SPRY), Lissencephaly type-1-like homology motif (LisH), carboxy-terminal to LisH motif (CTLH) and CT11-*RanBPM* (CRA motif) (reviewed by Murrin and Talbot, 2007). The structural organization of *RanBPM* suggests that it acts as a scaffolding protein for an array of signaling assemblies (Denti et al., 2004; Cheng et al., 2005 and Wang et al., 2002). Of interest to the current report is the role of *RanBPM* in regulating BDNF- triggered Trk-dependent MAPK and PI3K function (Yuan et al., 2006; Yin et al., 2010). Additionally, microarray analyses of cell lines reports that *RanBPM* down regulation modulates PI3K/AKT signaling (Atabakhsh et al., 2012). *RanBPM* has also been reported as a coordinator of signal inputs between lymphocyte function-associated antigen-1 (LFA-1) and intracellular signalling pathways involved in regulating immune function (Denti et al., 2004). A role for *RanBPM* phosphorylation has also been reported in the regulation of stress signaling pathways in response to extracellular stimuli such as UV and osmotic shock (Denti et al., 2004). Taken together these studies

support the hypothesis that *RanBPM* acts as a scaffolding protein in various signal transduction pathways.

1.2 *Drosophila RanBPM*

In *Drosophila, RanBPM* mutations cause pleiotropic phenotypes that include disruption of feeding, growth, response to light, locomotion resulting in late larval lethality (Scantelbury et al., 2010). Targeted expression of RanBPM in the nervous system, specifically in the mushroom bodies (MBs), rescues many of the phenotypes of *RanBPM* mutants including feeding behaviour (Scantelbury et al., 2010). Mushroom body is involved in olfactory learning and memory formation in insects e.g. honeybee, fly, cricket, grasshopper, locust, and cockroach (reviewed by McBride et al 2012). In line with these results, recent studies have shown that impairment of insulin signalling in the MB impairs feeding behaviour of the *Drosophila* larvae (Zhao and Campos, 2012). Studies examining the role of *RanBPM* in adult flies have demonstrated a requirement of *RanBPM* for the regulation of cell shape, size and organization of the germ line stem cell niche in the *Drosophila* ovary (Dansereau and Lasko, 2008). Our previous investigations have suggested a role for RanBPM protein in suppressing the neuromuscular junction overgrowth phenotype caused by mutations in *FMRP* gene known to be involved in the pathogenesis of fragile X syndrome (Scantelbury et al., 2010).

1.3 *Drosophila* fat body organ

The *Drosophila* fat body is a specialized tissue equivalent to the vertebrate liver and the white adipose tissue. This organ plays a central role in lipid storage and utilization (reviewed by Arrese and Soulages, 2010). It stores lipids as triacylglycerol and sugar as glycogen. Fat body acts as a central site for many metabolic processes including lipid, carbohydrate, amino acid and nitrogen metabolism. It behaves as an endocrine organ by producing and secreting several antimicrobial peptides (reviewed by Lemaitre and Hoffmann, 2007). The fat body coordinates systemic growth by controlling insulin-like peptide (ILP) secretion from the medial neurosecretory cells (mNSCs) upon a dietary stimulus of amino acids (Geminard et al., 2009). This occurs via a cationic amino acid transporter *slimfast (slif)* which mediates nutrient sensing by the fat body. Slimfast amino acid sensing in conjunction with Target of Rapamycin (TOR) signaling activate a fat body-derived signal that acts directly on the CNS to promote insulin secretion (Sousa-Nunes et al.,2011). Therefore, it is an important organ involved in integrating organism's response to various internal and external signals.

1.4 Insulin and Target of Rapamycin (TOR) signaling

Insulin and TOR pathways are both closely associated signaling cascades involved in metabolism and growth of an organism. There are seven dILPs that act on a single cell surface insulin receptor (InR) in *Drosophila*. The *Drosophila* InR is structurally and functionally homologous to mammalian InR/IGFR (reviewed by Oldham and Hafen, 2003). Sequence similarity between the fly and mammalian counterparts of the insulin

signaling pathway (i.e, insulin receptor and insulin receptor substrate) suggests that insulin system has multiple conserved roles (reviewed by Garofalo, 2002; Oldham and Hafen, 2003; Ullrich and Schlessinger, 1990). Ligand binding to Inr triggers an intracellular signalling cascade via the activation of phosphoinositide-3-OH kinases (PI3K) (Figure 1: Oldham and Hafen, 2003; reviewed by Grewal, 2009). Upon activation, PI3K phosphorylates inositol lipids to generate second messengers in the membrane. For example phosphatidylinositol-4,5-P_2 (PIP2) is phosphorylated to produce phosphatidylinositol-3,4,5-P_3 (PIP3) (reviewed by Rameh and Cantley, 1999). Phosphoinositide interacting domains referred to as the pleckstrin homology (PH) domains found in the cytoplasmic protein kinases such as the *Drosophila* homologue of Akt (also referred as protein kinase B, or PKB) and phosphoinositide-dependent protein kinase (PDK) are recruited to the plasma membrane via interaction with PIP_3 (Alessi et al.,1997; Gray et al., 1999). Recruitment to the plasma membrane and phosphorylation activates AKT (reviewed by Oldham and Hafen, 2003). *Drosophila* AKT has been identified as a cell- autonomous regulator of cell and organ size (Verdu et al., 1999). Activity of PI3K can be assayed using pleckstrin homology domain-green fluorescent protein (PH-GFP) fusion. PH-GFP is recruited to the cell membrane when PI3K activity is high and this localization can be visualized. Insulin/PI3K signaling in *Drosophila* is essential for coupling cellular metabolism with nutritional conditions (Britton et al., 2002). Cross talk exists between the insulin signalling components and the components

of Target of Rapamycin pathway (TOR) in controlling growth, ageing and autophagy (reviewed by Grewal 2009).

The TOR signaling pathway does not appear to function as a conventional linear signaling system (Raught et al., 2001). Rather both TOR and PI3K signaling are required for the activation or inactivation of downstream TOR proteins (Raught et al., 2001). Activation of AKT via insulin signaling is responsible for indirectly activating TOR signaling via S6K activation. S6K is a Serine/Threonine kinase involved in the translation of ribosomal proteins and translation factors (Reviewed by Oldham and Hafen, 2003). Additionally, AKT is also involved in inhibiting tumour suppressor genes (TSC1 and TSC2) and therefore positively signaling TOR pathway (Reviewed by Oldham and Hafen, 2003). TSC inhibits the regulatory kinase target of rapamycin (TOR) activity. In *Drosophila*, downstream effectors of TOR include a single initiation factor-4E-binding protein (*4E-BP*) homolog, *THOR/d4E-BP,* an inhibitor of the eukaryotic initiation factor 4E (eIF-4E). Together, the TOR/S6K signalling serves as an important regulator for cell and the overall growth in *Drosophila* (Oldham and Hafen, 2003).

TOR signaling cascade is also important for the regulation of autophagy. Autophagy is a process of cytoplasmic degradation that occurs in response to starvation to generate an internal source of nutrients (Scott et al., 2004). Under nutrient rich conditions, Ins/PI3K activity stimulates the TOR complex 1 which results in the activation of the downstream effectors of TOR and hence inhibits autophagy. Together, TOR and

Insulin signalling contribute in regulating key biological processes such as growth and autophagy.

1.5 Remote control of insulin secretion by the fat body

Recent studies have focused on the TOR dependent secretion of FDS for insulin secretion. Intercommunication between the fat body and DILP secretion via an unknown fat- body-derived signal (FDS) has been the central focus of questions concerning regulation of growth and neuroblast proliferation. Neuroblasts undergo a period of quiescence during the embryonic stages of development re-entering cell cycle post-embryonically. FDS has been shown to act directly on the CNS to allow neuroblast reactivation (Britton and Edgar, 1998). In *Drosophila*, the CNS contains two functionally segregated ILP pools, one that regulates proliferation of neural stem cells and the other that secrete insulin like peptides into the circulating hemolymph to promote systemic growth (Ikeya et al., 2002; Colombani et al., 2003, Sousa-Nunes et al., 2011). ILPs secreted from the mNSCs are involved in regulating systemic growth of the organism whereas ILPs, specifically dILP6, secreted from glial cells play a localized function in promoting neuroblast proliferation (Sousa-Nunes et al., 2011). IPCs along with adipokinetic hormone (AKH) producing cells (located in the ring gland) in the *Drosophila* brain are akin to α and β cells of the pancreas, respectively (Geminard et al., 2009). The IPCs express 4 of the 7 *Drosophila* insulin-like peptides (dILP 1, 2, 3 and 5). *dILPs* are expressed in a specific spatial, temporal pattern throughout development (Brogiolo et al., 2001). Expression of insulin like peptide 6 in the glial cells has been identified to

result in precocious reactivation of neuroblast under fed conditions. Consistent with this, the TOR/PI3K signaling in the glial cells was found to be sufficient for neuroblast reactivation (Sousa-Nunes et al., 2011).

Many studies have highlighted potential roles for hormones such as ALS, Imp-L2, NLaz, or Upd2 in the regulation of organismal growth (review by Hyun, 2013). Although mechanisms important for communication between fat body and CNS are not fully understood. Many important studies have unraveled the complex and integrative physiological network involved in regulating systemic growth and neuroblast cell-cycle re-entry.

1.6 Thesis objectives

The objective of my research project was to understand the role of *RanBPM* in the fat body for non-autonomous regulation of the starvation induced food intake, size, neuroblast proliferation and dILP accumulation (Figure 2). I have addressed this by asking the following questions:

Can all *RanBPM* mutant phenotypes be rescued by expressing *RanBPM* in the fat body? If so,

can all *RanBPM* mutant phenotypes be rescued by targeted overexpression of Ins/TOR components (eg. AKT, S6K, InR, TOR) in the fat body of *RanBPM* mutant larvae? Additionally, is autophagy (TOR dependent process) affected in the *RanBPM* null mutants? I expected to detect mis-regulation of autophagy in *RanBPM* mutants based on the observation of impaired systemic insulin signaling.

Chapter 2: Materials and Methods

Materials and Methods

2.1 *Drosophila* strains and culture

Synchronized early third instar foraging larvae of either sex were obtained as previously described [40] and grown at 29°C to maximize GAL4 activity, in light /dark cycle. Standard genetic crosses were used to construct stocks that allowed for the targeted the expression of transgenes (UAS constructs) under the control of GAL4 drivers in a homozygous RanBPM mutant background. The *RanBPM*^{K05201} allele was kept over a *CyO* (y+) balancer in a *yw* background for the identification of homozygous mutants by the mouth hook phenotype. Third chromosome constructs (GAL4 drivers or UAS constructs) were mostly kept over a TM6, Tubby (Tb), Stubbled (Sb) balancer chromosome. The target genes used were: UAS-*DILP2* kindly provided by Ernst Hafen, UAS-RanBPM (short isoform) stock kindly provided by Paul Lasko, UAS-*DILP6* kindly provided by Michael O'Connor, w[1118]; P{w[+mC]=UAS-GFP.nls}8 (Bloomington stock center (BSC# 4776), P{w[+mC]=UAS-Akt1.Exel}1, y[1] w[1118] (BSC# 8192), y[1] w[1118]; P{w[+mC]=UAS-InR.A1325D}2(BSC# 8263), y[1] w[1118]; P{w[+mC]=UAS-InR.K1409A}3 (BSC# 8253), w[1118]; P{w[+mC]=UAS-S6k.STDE}3 (BSC#6913), y[1] w[*] P{ry[+t7.2]=hsFLP}1; P{w[+mC]=UAS-Tor.WT}3 (BSC# 7012). The GAL4 drivers used were: *Lsp2*-Gal4 expressed in the larval fat body beginning in the early third instar, (Yang and Berggren, 2006 ; Moncalvo and Campos, 2009) (BSC#6357), *C929*-GAL4 reflecting the expression of the transcription factor Dimmed required for the NS cell fate (BSC# 25373) (Grewal, 2009; Teleman, 2010), *DILP2*-GAL4 kindly provided by Ernst Hafen (Sousa-Nunes et al., 2011)

and *repo*-GAL4 expressed in all glia throughout embryonic and post embryonic development (BSC# 7415) (Lazareva et al., 2007; Sepp et al., 2001).

2.2 Feeding behaviour assay

The assay was as described previously (Awasaki and Ito, 2004) for adult flies with some modifications. Batches of 60-70 newly hatched larvae (0-60 min) were transferred to regular food plates (30 X 13 mm Fisher) and kept at 29° C for 41-46 hours. Sixty larvae were recovered from the food plate, washed and transferred onto a damp 3M filter paper placed in a Petri dish (humid chamber) and starved for 2.5 hours. Larvae were then transferred to a drop of freshly prepared yeast paste (5 g in 15 ml) containing 3.3% FD&C Blue No.1 [McCormick] and left for 1.5 hours. Control constituted matched larvae (age and genotype) fed in yeast with no dye. At the end of this period larvae were washed, homogenized and centrifuged twice (15 min X 13000 G). The supernatants were transferred to cuvettes and the absorbance was measured at 625 nm using as a blank extracts from control larvae. All larval cultures were kept at 29° C, which is the optimum temperature for the yeast GAL4. For all genotypes a minimum of three independent assays with 60 larvae each were conducted.

2.3 Statistical Analyses

All statistical tests were conducted using the MINITAB Student software package (student release version 14.11.1). The statistical tests included one-way analysis of

variance (ANOVAs) and Tukey's pairwise comparisons. Normality tests on the residuals of the ANOVAs were conducted using the Shapiro-Wilk test. The level of significance in all tests was 0.05. All measurements are shown as mean values and SEM and * indicates samples that are significantly different from control genotypes.

2.4 Immunohistochemistry and Imaging

CNS dissected from early foraging third instar larvae staged as above were treated as described (Iijima et al., 2009). Primary antibodies used were rabbit anti-phosphorylated Histone3 (Upstate Biotechnologies 1:500), and anti-DILP2 kindly provided by Ernst Hafen (1:200). The secondary antibody used was a Alexa 488-conjugated goat anti-rabbit IgG (1:200). In the case of DILP2 immunolabelling mutant and wild type specimens were incubated in the same tube to avoid variability in antibody concentration. The genotype of the specimens was distinguished by the presence or absence of the yellow (y) marker in the mouth hooks and by the size of the dissected brain. All RanBPM mutant brains were smaller than age-matched controls. In order to estimate the relative amount of DILP2 present in the brain IPCs confocal Z stacks at 1 µm steps were obtained using identical laser power and scan settings adjusted to below saturation using the wild type samples. ImageJ software was used to measure fluorescent intensity of the cell bodies as described in (Arrese and Soulages, 2010). We used a Leica Confocal microscope SP5II. Brightness and contrast were adjusted using Adobe Photoshop.

2.5 Western blotting analysis

Protein lysates were prepared typically from 20-30 3rd instar foraging larvae synchronized as described above, homogenized by douncing in SDS sample buffer and a cocktail of protease and phosphatase inhibitors (Fisher Scientific #PI78441). Western blotting analysis was performed as described before (Hassan et al., 2005), using commercially available antibodies for AKT (Cell Signaling #4691), *Drosophila* phospho-Ser505 AKT (Cell Signalling, #4054) and actin (Millipore #MAB1501R) at a 1 to 1000 dilution according to the manufacturer's protocol.

2.6 Lysotracker staining and imaging of fat body

Synchronized late third instar larvae were first removed from food culture and transferred by forceps to small dishes containing 3M filter paper saturated with water for 4.5 hours to induce starvation. Alternatively, the larvae removed from the food culture were dissected to extract the fat body for subsequent staining process. LysoTracker Red DND-99 (Molecular Probes) was diluted in PBS to obtain a 50 µM solution for staining. Dissected fat body samples were incubated in 50 µM LysoTracker Red DND-99 solution for 2 minutes and then mounted on a microscope slide in 1Xs PBS solution, and covered with a coverslip for imaging. Samples were quickly examined using confocal microscopy.

2.7 Data organization for figures

Figures 3 to 16 were labeled using Photoshop software. Raw data used to create graphs was first analyzed using Minitab software and then plotted using CricketGraph (graphic software for the Apple Macintosh). Graphs were labelled using Photoshop software.

Chapter 3: Results

Results

3.1 Targeted expression of *RanBPM* in neurosecretory cells rescues the disruption in feeding behaviour, reduced growth and lethality of *RanBPM* mutants

In an attempt to identify the cells in which *RanBPM* plays a role we screened for promoters (*GAL4* drivers) capable of rescuing *RanBPM* phenotypes when regulating the expression of *RanBPM* cDNAs in a mutant background. We found that the *C929-GAL* driver reflecting the expression of the *dimmed* (*dimm*) gene, is capable to rescue all phenotypes as seen by the rescue of larval lethality and the eclosion of 83% of the expected homozygous mutant progeny (N=607). The eclosed flies were of normal size and morphology (Additional file 1). Consistent with these observations we found that the feeding behaviour phenotype was similarly restored (Figure 3). Amongst the C929-positive cells are the insulin producing cells located pars intercerebralis of the brain and the corpora cardiaca located in the ring gland expressing the adipokinetic hormone (AKH), the *Drosophila* Glucagon and the fat body, the *Drosophila* equivalent of the vertebrate liver and white adipose tissue (Park and Tagert, 2009; Park et al., 2008; reviewed by Arrese and Soulages, 2010).

3.2 *RanBPM* gene function is required for proper insulin gene expression and secretion

Amongst the best-studied DIMM positive cells are the insulin producing cells located in the pars intercerebralis region of the brain lobes which together with the AKH producing cells of the ring gland constitute a primitive *Drosophila* bipartite pancreas. Therefore we sought to determine whether these cells were affected by *RanBPM* mutations. To that end, we used the targeted expression of Green Fluorescent Protein (GFP; UAS-GFP:LacZ.nls) under the regulation of the *C929-GAL4* driver to visualize the C929 positive neurosecretory cells in *RanBPM* mutants and in wild type control specimens.

At gross level, the overall distribution and number of C929 positive clusters were not disrupted by *RanBPM* mutations in spite of the reduced size of the *RanBPM* mutant brain (Additional file 2). We focused on the subset of C929 cells located in the pars intercerebralis, the medial neurosecretory cells (mNSC) cluster. It consists of circa 15 cells and includes the 7 insulin producing cells (Figure 5A) (Park and Tagert, 2008). The position and arrangement of this cluster in *RanBPM* mutant brains differed little from that found in wild type control specimens (Figure 5B). The number of cells in this subset was significantly smaller in *RanBPM* mutant samples (Additional file 3). In contrast, the number and arrangement of the AKH producing cells visualized by the expression of GFP under the regulation of *AKH-GAL4* driver were not affected by *RanBPM* mutations (Figure 5C and D and Additional file 3).

The larval insulin producing cells express three (*DILP 2, 3* and *5*) of the 7 *DILPs* genes found in the *Drosophila* genome (Ikeya et al., 2002). Of these, *DILP2* is the most abundantly expressed, estimated to comprise 80% of DILP gene expression in these cells (Buch et al., 2008). *DILP2* is the first to be expressed during larval development from the first instar on and, in contrast to *DILP3* and *5*, the level of *DILP2* RNA is not regulated by nutrient availability (Ikeya et al., 2002). In order to evaluate the requirement for *RanBPM* gene function for the expression of the *DILP2* gene we introduced *DILP2* reporter constructs (*DILP2*-GAL4; *UAS-GFP*) in *RanBPM* mutant larvae. We found that in foraging third instar larvae homozygous for a null mutation in the *RanBPM* gene, expression of *DILP2*-GAL4 could not be detected at the level of resolution afforded by confocal microscopy (Figure 5E and F) suggesting that at that stage in larval development the transcription of DILP2 gene requires *RanBPM* gene function.

Starvation causes the increased accumulation DILP 2 and 5 peptides in the brain insulin producing cells to levels above that of fed larvae suggesting an inhibition of secretion (Geminard et al., 2009). Therefore, we asked whether the level of DILP2 in the insulin producing cells of the third instar larva is affected by mutations in the *RanBPM* gene. To that end we used a polyclonal antibody against DILP2 (kindly provided by Ernst Hafen) to immunolabel dissected CNS from wild type and *RanBPM* mutant foraging third instar larvae. In order to obtain confocal images that would allow us to make a semi-quantitative comparison, we used wild type specimens to establish laser and scan settings below saturation to be used in all mutant specimens. Representative

photomicrographs of brains imaged in this manner and a graph depicting the relative fluorescence intensity are shown in Figure 5A and B respectively.

We found that in third instar *RanBPM* mutant larvae in spite of the marked reduction in the expression of the *DILP2-GAL4* reporter the insulin producing cells showed a 2,5 fold higher level of *DILP2* peptide than that of wild type samples (Figure 5B). The number of *DILP2* positive cells however did not appear to be affected in *RanBPM* mutants. In contrast, in the second instar larva the level of *DILP2* measured as described above is comparable to that of wild type control specimens (Additional file 4).

Taken together these observations demonstrate that *RanBPM* gene function is required for proper expression of the *DILP2* gene at the level of transcription in the third instar larva inferred from the lack of expression of the *DILP2-GAL4* reporter. Our results suggest that concomitant to the reduced expression of the *DILP2* gene, the steady state level *DILP2* peptide insulin producing cells is above the level found in wild type specimens suggesting that secretion is inhibited. Whether the apparent reduction in DILP2 secretion is a direct effect of lack of *RanBPM* function or an indirect consequence of starvation was not addressed by these experiments.

3.3 *RanBPM* mutants display reduced peripheral insulin signalling

The results described above indicate that in *RanBPM* mutants the level of circulating insulin is reduced and that may be the cause of the reduced growth and feeding of the third instar larva. In order to test this hypothesis we analysed the phosphorylation status of dAKT one of the major kinases activated upon InS. Immunoblots of phospho-AKT (pAKT), total AKT using whole larval extracts indicated that while the steady state level of total AKT was not affected in *RanBPM* mutants the level of pAKT is markedly reduced in these larvae (Figure 5C and Additional file 5).

To further confirm the impact of *RanBPM* mutation on InS we used a GFP-pleckstrin homology domain (PH) fusion regulated by the Tubulin promoter (TGPH) construct as a reporter for InR/PI3K activity (Britton et al., 2002). The GPH fusion protein accumulates in the plasma membrane of various cell types when InR/PI3K signalling is activated (Britton et al., 2002). Consistent with the previous observation of an overall reduction in dAKT activation, we found that in the salivary glands and fat body cells of *RanBPM* mutants GPH is found predominantly in the cytoplasm, in marked contrast to matched wild type control samples in which GPH labelling accumulates at the plasma membrane (Figure 5D). Taken together these observations support the notion that *RanBPM* function is required in the foraging third instar larva for systemic InS.

3.4 Forced expression of *DILPs* suppresses the feeding, size and CNS proliferation phenotypes of *RanBPM* mutants

The results presented above suggest that the *RanBPM* phenotypes are due to impaired InS likely due to reduced *DILP2* expression and secretion. In order to further test this hypothesis we asked whether any of the *RanBPM* phenotypes can be modified by over expression of *DILP2* achieved through the GAL4/UAS system. To that end, we used various GAL4 drivers to activate the expression of the *UAS-DILP2* transgene in a *RanBPM* mutant background. We chose a strong ubiquitous driver, *tub-GAL4* and *c929-GAL4* expressed in the NS cells that include the insulin producing cells and the fat body.

Recent reports established that forced expression of DILP2 or DILP6 under the regulation of *repo-GAL4* is sufficient to by pass the nutritional requirement for neuroblast re-entry into the cell cycle during larval development (Sousa-Nunes et al., 2011; Chell and Brand, 2010). *RanBPM* mutants display a marked reduction in CNS proliferation as seen by reduced immunolabelling of a phospho specific isoform of Histone 3 (phospho H3) however *RanBPM* expression was not detected in these cells suggesting that this is a non-autonomous phenotype (Scantelbury et al., 2010). Therefore we also used *repo-GAL* to up-regulate DILP2 and DILP6 in the glia of *RanBPM* mutant larvae in order to establish whether in these mutants reduction of glia-derived insulin is the cause of the observed reduced proliferation in the CNS.

Null mutations in the *RanBPM* gene are strict late larval lethals (Scantelbury et al., 2010). Over expression of *DILP2* under the regulation of any of the GAL4 drivers employed or DILP6 under the regulation of *repo-GAL4* was not sufficient to rescue the lethality of *RanBPM* mutants, as adults were never recovered in various experiments. However, ubiquitous over expression of *DILP2* under the regulation of tub-GAL4 allowed for 64% (N=160) of *RanBPM* mutant larvae to reach the pupal stage.

We found that in *RanBPM* mutant larvae over expressing *DILP2* dye accumulation in the gut was significantly higher than in mutant controls (Figure 6A). These larvae were in general bigger than the sibling mutant controls (Figure 6B). In contrast, forced expression of *DILP2* or *DILP6* under the control of the pan glial driver *repo-GAL4* did not increase the level of dye in the gut or the size of *RanBPM* mutants (Figure 6A and data not shown). Ubiquitous over expression of *DILP2* in a wild type back ground did not significantly change dye accumulation suggesting that the increase observed in mutants overexpressing *DILP2* under the regulation of the same promoter (*tub-GAL4*) is due to the restoration of reduced level of systemic insulin.

The reduced size and CNS proliferation phenotype of *RanBPM* mutants was also suppressed by the ubiquitous overexpression of *DILP2* under the control of the *tub-GAL4* element (Figure 6C). In the *RanBPM* mutants the eye-antennal imaginal disc is rarely visible (Figure 6C). Over expression of *DILP2* was sufficient to rescue the eye disc growth deficiency (arrowhead in Figure 6C). Expression of *DILP6* under the control of *repo-GAL4*

was sufficient to bypass the reduced CNS proliferation characteristic of *RanBPM* mutants but not the reduced size of the eye imaginal disc (Figure 6C), suggesting that lack of *RanBPM* gene function disrupt the glial derived insulin regulation of CNS proliferation.

Combined these results demonstrate that InS is impaired by lack of *RanBPM* function and suggest that this is at least in part due to the reduced level of systemic DILP2. Moreover our observations support the hypothesis that *RanBPM* function contributes to the role of glia as the source of insulin required for the reactivation of quiescent neuroblasts. The results presented here do not exclude the possibility that reduced function of the other *DILPs* expressed by the insulin producing cells and elsewhere in the larva may be also impaired by the *RanBPM* mutation.

3.5 Targeted expression of *RanBPM* in the fat body partially rescues most of the *RanBPM* mutant phenotypes

The fat body has emerged as a crucial organ in the coordination of growth with nutrient availability in *Drosophila* [e.g. (Colombani et al., 2003); see commentary in [Rajan and Perrimon, 2011)]. Recent reports elegantly demonstrate that fat body-derived factors regulate glial DILP6 and DILP2 expression required for the reactivation of the neural stem cells in the *Drosophila* larval brain (Chell and Brand, 2010; Sousa Nunes et al., 2011). Similarly, DILP secretion by the brain insulin producing cells is regulated remotely by the fat body (Geminard et al., 2009). These observations together with the

finding that expression of c929-GAL4 element is found in the fat body (Park et al., 2008) prompted us to ask whether targeted expression of *RanBPM* in this organ is sufficient to rescue any of the *RanBPM* mutant phenotypes. To that end we took advantage of two fat body GAL4 drivers with different onsets of expression in this organ. *Pumpless* (*ppl*)-*GAL4* is expressed in the fat body throughout larval development with the expression of *ppl* decreasing near the end of third instar (Zinke et al., 1999). Reports have established that expression of *ppl* occurs in a mosaic pattern (Bi et al., 2012). While *Larval serum protein 2(Lsp2)*-GAL4 driver has been reported in studies to be active during the third larval stage (Reiling and Hafen, 2004; Aguila et al., 2007).

Indeed, we found that the feeding behaviour and growth deficits of *RanBPM* mutant larvae in which expression of this gene was restored to the fat body using either one of the GAL4 drivers, were partially rescued (Figure 7 A and B and Additional file 6). These observations were confirmed by RNAi knock down of *RanBPM* restricted to the fat body using both GAL4 drivers significantly reduced dye accumulation in the gut and disrupted larval growth (Additional file 7). The reduced CNS proliferation phenotype is similarly suppressed by targeted expression using either GAL4 driver (Figure 7E). Finally, we did not detect the characteristic increased accumulation of DILP2 immunofluorescence in the insulin producing cells in *RanBPM* mutant larvae in which expression of this gene was restored to the fat body (Figure 7C). Similar results were obtained when *ppl*-GAL4 was used to drive the expression of *RanBPM* cDNA (Figure 7D).

This indicates that expression of *RanBPM* regulates insulin accumulation in the brain non-autonomously.

Taken together these results support the notion that *RanBPM* gene function contributes to the regulated expression and secretion of *DILP2* from the insulin producing cells in the brain and that this is carried out at least in part through its function in the fat body. Moreover *RanBPM* function in the fat body contributes to the remote regulation of CNS proliferation and feeding behaviour either directly or indirectly through regulation of insulin.

3.6 Overexpression of AKT in the fat body partially rescues *RanBPM* mutant phenotypes

Previous observations showed an increased level of *DILP2* peptide in the IPCs of the *RanBPM* mutants compared to wild type control specimens suggesting that secretion was inhibited (Figure 7A). Indeed a general reduction of the phosphorylated *AKT* and the membrane localization of tGPH reporter were detected in the fat body and salivary gland of *RanBPM* mutants (Figure 7D). These observations suggest that circulating insulin is reduced in *RanBPM* mutants. Therefore we asked whether overexpression of DILP using various GAL4 drivers was sufficient to suppress *RanBPM* mutant phenotypes. Ubiquitous expression of DILP2 using tub-GAL4 driver suppressed feeding, size and CNS proliferation phenotypes of *RanBPM* mutants (Figure 6). As

discussed earlier, the fat body in *Drosophila* has emerged as an important organ involved in coupling growth with nutrient availability. The fat body has been proposed as a regulator of DILP secretion from the IPCs (Geminard et al., 2009; Colombani et al., 2003). In conjunction to these reports, our investigations demonstrated that targeted expression of *RanBPM* gene exclusively in this organ was sufficient to restore the food intake, growth deficit, neuroblast proliferation and dILP accumulation phenotypes of the *RanBPM* mutants (Figure 7). Taken together these observations suggest that *RanBPM* phenotypes are the result of impaired InS likely due to the requirement of *RanBPM* in the fat body for the regulation of DILP2 expression and secretion from the IPCs.

Inhibition of TOR signaling in the fat body and dietary restriction leads to DILP2 retention in the IPCs of the larval brain (Geminard et al., 2009). This demonstrates the requirement of a TOR dependent mechanism in the fat body for the fat body derived humoral factor in regulating insulin secretion from the IPCs. TOR kinase can be activated either directly via nutritional input or by *AKT* activation. Therefore, we investigated a role for *AKT* within the fat body of *RanBPM* mutants for the remote control of DILP secretion. To that end we asked whether up-regulation of *AKT* targeted to the fat body using *Lsp2*-GAL4 or *ppl*-GAL4 drivers has an impact on various *RanBPM* phenotypes.

I found that the targeted overexpression of *AKT* using *Lsp2*-GAL4 driver partially restored some of the *RanBPM* mutant phenotypes (Figure 8). Overexpression of *AKT* using *Lsp2*-GAL4 in *RanBPM* mutant larvae showed a significant increase of dye accumulation in the gut compared to the parental controls (*RanBPM*^{K05201}; *Lsp2*-GAL4/+

and UAS-*AKT*;*RanBPM*^{K05201}) (Figure 8A). However the level of dye in the gut was not as high as the level of accumulation detected in the WT control larvae. Previous observations showed that *RanBPM* mutant larvae that expressed *RanBPM* gene in the fat body under the control of *Lsp2*-GAL4 was sufficient to significantly increase the level of dye in the gut compared to parental controls and that is indistinguishable from the WT control(Figure 7A). When *ppl*-GAL4 driver was used to express the *RanBPM* cDNA in *RanBPM* mutant larvae the level of absorbance at 625nm was indistinguishable from the WT control despite the finding that the mean absorbance was lower compared to the mean absorbance achieved under the regulation of *Lsp2*-GAL4 (Figure 7A). However, when *ppl*-GAL4 was used to drive the expression of *AKT* in the *RanBPM* mutants the level of dye in the gut was not statistically different from the parental controls (Figure 8E). Reports have established that expression of *ppl* decreases near the end of third instar (Zinke et al., 1999) and that expression of *ppl*-GAL4 occurs in a mosaic pattern (Bi et al., 2012). In contrast to this, *Lsp2*-GAL4 driver has been reported in studies to be active during the third larval stage (Reiling and Hafen, 2004). Together, with the finding that overexpression of *AKT* under the control of *ppl*-GAL4 did not rescue the feeding phenotype in the *RanBPM* mutants suggests that expression of *AKT* did not reach the required threshold to restore the feeding behaviour. The size of the larvae expressing *AKT* under the regulation of *Lsp2*-GAL4 appeared bigger compared to *RanBPM* mutants (Figure 8B). Most of these larvae appeared similar in size to their parental control (*RanBPM*^{K05201}; *Lsp2*-GAL4/+) suggesting that the overall growth of the larvae expressing

AKT under the regulation of *Lsp2*-GAL4 was partially rescued. In contrast, the larvae expressing *AKT* under the control of *ppl*-GAL4 did not appear bigger in size compared to the *RanBPM* mutants (data not shown).

DILP2 immunolabeling of *RanBPM* mutant larval CNS expressing *AKT* under the control of *Lsp2*-GAL4 was done to determine whether increased level of dILP2 in the IPCs was ameliorated. Indeed, targeted expression of *AKT* in the fat body resulted in a lower level of DILP2 in the IPCs compared to *RanBPM* mutant control (Figure 8C and 8D). However, the level of DILP2 detected in these larval IPCs was still significantly higher than the WT control larvae. Whereas, previous observations of DILP2 immunolabeling showed that the *RanBPM* mutant larvae which expressed *RanBPM* gene under the regulation of *Lsp2*-GAL4 resulted in level of DIL2 accumulation that was indistinguishable from the WT control larvae (Figure 7C and 7D). AKT overexpression using either *Lsp2*-GAL4 or *ppl*-GAL4 appeared to increase the number of phospho-H3 labelled cells in the brain lobes and the ventral nerve cord of *RanBPM* mutants (Figure 8E). The increase in the phospho-H3 labeling detected in the CNS here does not appear to be different between the two promoters used. The overall pattern of the phsopho-H3 labeling in these *RanBPM* mutant larvae expressing *AKT* under the regulation of *Lsp2*-GAL4 or *ppl*-GAL4 was similar compared to the WT control. However, in these *RanBPM* mutant larvae expression of *AKT* under the regulation of *Lsp2-GAL4* or *ppl*-GAL4 did not cause a change in the size of the CNS as compared to the *RanBPM* mutant control. These observations show that although the pattern of phsopho-H3 labeling was partially

rescued the CNS size of these larvae remained smaller compared to the WT control. In previous experiments when *Lsp2*-GAL4 or *ppl*-GAL4 was used to drive the expression of *RanBPM*, these constructs were sufficient to rescue most of the *RanBPM* mutant phenotypes (Figure 7). However in *RanBPM* mutants when *AKT* is overexpressed under the regulation of *Lsp2*-GAL4, the CNS proliferation, DILP accumulation and the feeding are partially restored to the WT conditions (Figure 8). Whereas, when *AKT* is overexpressed under the regulation of *ppl*-GAL4 the feeding (Figure 8A) and the larval size phenotypes (data not shown) of the *RanBPM* mutants were not rescued. This suggests that *AKT* might not be providing expression close to the threshold to induce a change in the feeding and the size phenotypes of the *RanBPM* mutants.

The results presented above indicate that targeted expression of *AKT* in the fat body can partially rescue food intake, size, CNS proliferation and insulin secretion phenotypes of *RanBPM* mutants. Based on these results, we wanted to investigate whether components of insulin signaling pathway that are upstream of *AKT* such as *InR* can also modify any of the *RanBPM* mutant phenotypes. To investigate this, I used a constitutively active construct of insulin receptor (*UAS-InR* (*CA*)) under the regulation of the *Lsp2*-GAL4. I found that expression of this construct in *RanBPM* mutants did not rescue the feeding phenotype (Figure 8A) or the phospho-H3 labeling of the CNS (compare Figure 10B to 10C).

Since previous observations showed that targeted expression of *AKT* under the regulation of *Lsp2*-GAL4 and *ppl*-GAL4 had an impact on various *RanBPM* mutant

phenotypes, I also expressed myristoylated AKT in the fat body using the same promoters. The feeding phenotype was not rescued when *AKT (myr)* was expressed under the regulation of *Lsp2*-GAL4 or *ppl*-GAL4 (Figure 9A). The size phenotype was not rescued in *RanBPM* mutants expressing *AKT* (*myr*) under the control of the *ppl*-GAL4 (Figure 9B). Myristoylation targets the protein to the membrane rendering it unable to interact with cytosolic and nuclear proteins thus impairing its mediation of insulin receptor activation.

3.7 Up-regulation of Target of Rapamycin (TOR) or S6K in the fat body of *RanBPM* mutants partially rescues the CNS proliferation phenotype of *RanBPM* mutants

Studies carried out in *Drosophila* indicate that *TOR* signaling is the major pathway in the fat cells that relays the nutritional signal to brain IPCs via the secretion of yet unidentified fat body derived factor (Geminard et al., 2009; Colombani et al., 2003). To study the role of *TOR* signaling in the fat body of *RanBPM* mutants, I up-regulated the expression of wild type *TOR* gene (UAS-*TOR*) and of a constitutive active form of the *S6K* (UAS-*S6K* (CA)) under the control of *Lsp2*-GAL4 and *ppl*-GAL4 drivers. Up regulation of *TOR* using *Lsp2*-GAL4 in the *RanBPM* mutants showed an increase in the phospho-H3 labeling of the CNS for most of the samples visualized (Figure 11C). However, rest of the samples did not shown an increase in the phospho-H3 labeling of the CNS when *TOR* was up- regulated under the control of *Lsp2*-GAL4 in *RanBPM* mutants (Figure 11D). These observations suggest that CNS proliferation phenotype was only partially rescued. *TOR*

up-regulation in the fat body did not appear to cause an increase in the size of the CNS compared to *RanBPM* mutants (compare Figure 11B to 11C and 11D). Overexpression of *TOR* under the control of *ppl*-GAL4 driver was not performed due to time constraints. *S6K* overexpression under the regulation of *Lsp2*-GAL4 and *ppl*-GAL4 drivers increased the phospho-H3 labelling in the thoracic ventral cord region of the CNS (Figure 12). The overall pattern of the phsopho-H3 labelling in the *RanBPM* mutants expressing *S6K* under the control of *Lsp2*-GAL4 or *ppl*-GAL4 appeared similar to the phsopho-H3 labeling of the WT CNS (compare Figure 12A to12C and 12D). Indeed the CNS size of these larvae appears bigger than the *RanBPM* mutant control however the size is not comparable to the CNS of the WT control. Taken together these observations suggest that the CNS proliferation and the CNS size phenotypes of third instar *RanBPM* mutant larvae was only partially rescued when *S6K* was overexpressed in the fat body (Figure 12). The overall size of the *RanBPM* larvae overexpressing *S6K* under the control of *Lsp2*-GAL4 was bigger in comparison to *RanBPM* mutants suggesting that size phenotype was partially rescued (Figure 12E).

3.8 Autophagy in *RanBPM* mutants

Autophagy, a cellular response to starvation, is an evolutionarily conserved mechanism of bulk degradation to match the supply of nutrients with the cell's demand for energy. Scott et al, have shown that autophagy is rapidly induced in the fat body of *Drosophila* larvae in response to nutrient withdrawal by examining the autolysosomal

content of the fat body cells. Fluorescent dyes such as Lyso Tracker Red or transmission electron microscopy can be used to observe autolysosomal structures in the fat body(add a reference here).

Autophagy is regulated by the nutrient sensing pathway, TOR (reviewed by Grewal, 2009). TOR inactivation is known to trigger autophagy despite nutrient availability in rat hepatocytes (Blommaart et al., 1995). Studies in vertebrates have also shown that starvation-induced autophagy can be suppressed by activating InR, PI3K and Akt (Petiot et al.,2000).

Previous observations indicated that *RanBPM* phenotypes are a result of impaired insulin signaling. Consequently, restoring *RanBPM* gene function in the fat body suppressed *RanBPM* mutant phenotypes. As discussed earlier, TOR signalling plays an important role in the fat body in the control of the autophagic machinery. To determine whether autophagy is mis-regulated in *RanBPM* mutants, I used Lyso Tracker Red to label autophagosomal structures in the fat body of fed and starved larvae. Consistent with the literature, I found increased punctate staining in the fat body of the starved wild type (yw) larvae in comparison to fed conditions (Figure 14 A and C). I compared the level of autophagy in the *RanBPM* mutant fat body under starved and fed conditions. In the *RanBPM* mutants, lysosomes were only detected in starved conditions (Figure 14). This suggests that in *RanBPM* mutants, starvation triggers autophagy (Figure 14). Starvation causes a reduction in fat body cell size (Butterworth et al., 1965) and stimulates lipid mobilization which results in lipid droplet aggregation (Britton et al.,

2002; Zhang et al., 2000). Lipid droplet aggregation was estimated by measuring the diameter of the unstained lipid droplets in the fat body cells. In both the WT control and the *RanBPM* mutants, 4.5 hours of starvation showed an increase in the diameter of the lipid droplet size (Figure 15A and 15B). The increase in the size of the lipid droplets is likely due to the result of lipid droplet aggregation. Similar to fed conditions, the lipid droplet size after starvation was smaller in *RanBPM* mutants compared to the wild type control. Lysotracker staining of the *RanBPM* mutants suggests that perhaps the cellular machinery involved in activating autophagy (ie. TOR and ATG-1) is not disrupted by *RanBPM* mutation.

3.9 Up-regulation of insulin signalling in the fat body

Past studies have shown that overexpressing insulin receptor under the regulation of *ADH-GAL4* induces larval wandering away from food (Britton et al., 2002). *ADH-GAL4* is known to be expressed in the fat body, trachea, and few cells of the gut. This prompted use to ask whether up-regulation of insulin signaling in the fat body is sufficient to inhibit the starvation dependent food intake observed in third instar foraging larvae. This was achieved by driving the expression of insulin signaling components using fat body specific *Lsp2-GAL4* driver. The insulin signaling components that were used included *Akt (myr), S6k (CA),* wild type *Akt*, *InR(DN)* and *InR(CA)*. Feeding assays (described in the methods section below) were conducted using *Drosophila* late third instar larvae of the various genotypes to determine the starvation dependent food

intake response. Overexpression of the insulin signaling components using *Lsp2-GAL4* did not inhibit the starvation dependent food intake (Figure 12). This can be explained by considering that perhaps the expression was not sufficient enough to reach a required threshold to induce a response in feeding.

Chapter 4: Discussion

Discussion

There has been a renewed interest in research surrounding regulation of growth and size via inter-organ communication. Research in the field of metabolic regulation has been of interest in the recent years because of the growing world-wide epidemic of type 2 diabetes and obesity. Insulin and TOR signaling network pathways play a central role in regulating metabolism. Here, I report studying the role of these pathways in the regulation of growth and behavior in the model organism, *Drosophila*. Over the past decade, *Drosophila* has become an important model system to study Ins/TOR signaling mechanisms because genetic tools available in *Drosophila* allow researchers to conduct loss-of-function and genetic interaction experiments to gain a better understanding of genetic relationships (reviewed by Teleman, 2010). Additionally, conservation of genes and signaling pathways between mammals and *Drosophila* makes the latter an important model system for studying InS/ TOR signaling.

Drosophila progresses through three critical developmental stages throughout its life cycle. Beginning as a developing embryo, *Drosophila* hatches as a larva which develops through three instar stages and undergoes metamorphosis before emerging as an adult fly. During the larval stages of development, growth increase is nutrient dependent. Larval and imaginal tissues increase in mass during this developmental period. Internal, physiological signals in addition to external cues are involved in regulating larval growth (reviewed by Mirth and Shingleton, 2012).

Drosophila insulin like peptides functions to couple growth with changes in nutritional availability by a fat body-dependent mechanism. ILPs secreted from the IPCs are released into the hemolymph and act to promote growth by activating insulin receptor systemically. The *Drosophila* fat body, vertebrate homolog of liver and white adipose tissue, controls insulin secretion from the IPCs in a TOR-dependent mechanism. Understanding the mechanisms involved in signaling between the *Drosophila* fat body and the brain will provide further insight into the regulation of growth and size.

This report presents evidence for the role of *RanBPM* in the fat body for the proper expression and secretion of insulin (DILP2) from the brain IPCs in regulating size and feeding behaviour of *Drosophila* larvae. I also present evidence for the role of *DILP6* from the glial cells in the *RanBPM* mutants for the regulation of CNS proliferation. Additionally, genetic epistasis experiments were performed to investigate the role of InS/TOR signaling in *RanBPM* mutant phenotypes in the fat body for the remote control of DILP secretion.

4.1 *Impaired insulin signaling in RanBPM mutants*

Fat body- dependent remote control of insulin secretion through a TOR dependent mechanism has been previously reported (Geminard et al., 2009). Inhibition of the TOR signaling pathway in the fat body or starvation induces dILP retention in the IPCs consequently restricting larval growth (Geminard et al., 2009). We found an increased level of *dILP2* in the IPCs of the *RanBPM* mutant larvae (Figure 5A and 5B).

This is supported by reduced membrane localization of TGPH in the fat body and salivary glands in addition to reduced *AKT* activation in *RanBPM* mutants. Reduced levels of systemic insulin signaling suggest that dILP secretion is inhibited from the IPCs. Furthermore, ubiquitously over expressing *DILP2* in *RanBPM* mutants resulted in the rescue of the mutant phenotypes. These observations suggest the requirement of *RanBPM* function either upstream or downstream of insulin signaling.

4.2 *Expression of RanBPM in the fat body*

To investigate whether targeted expression of *RanBPM* in the larval fat body, a central link between Ins/TOR signaling and insulin secretion from brain IPCs, is sufficient to rescue *RanBPM* mutant phenotypes Lsp2-GAL4 and ppl-GAL4 drivers were used to restore the function of this gene. Indeed, targeted expression was sufficient to improve food intake, growth, and restore the level of DILP2 in the IPCs of *RanBPM* mutants. However, late third-instar lethality phenotype caused by *RanBPM* mutation was not rescued. In contrast, when *RanBPM* gene was expressed under the regulation of C929-GAL4 driver in *RanBPM* mutants, lethality was suppressed. Homozygous *RanBPM* mutants survived to adulthood and were normal in size and appearance. The expression of *C929*-GAL4 reflects the expression pattern of DIMMED transcription factor, which includes CNS cells and peripheral cells (ie. fat body) (Park et al., 2008). These observations suggest the requirement of *RanBPM* in both peptidergic neurons and the fat body to overcome lethality.

Previous studies have reported the role of glial cells as the source of ILP6 for neuroblast reactivation during the late first instar stage of the *Drosophila* larva (Sousa-Nunes et al., 2011). Whereas ILPs secreted into the hemolymph from medial neurosecretory cells control organismal size (Brogiolo et al., 2001; Ikeya et al., 2002). To address whether glial derived *ILP6* is sufficient to rescue CNS proliferation in *RanBPM* mutants DILP6 was expressed in the glial cells. CNS proliferation was restored when *DILP6* was overexpressed in *RanBPM* mutants under the control of pan glial driver, *repo*-GAL4. This suggests that lack of *RanBPM* function disrupts glial derived ILP6 regulation. Conversely, overall growth and food intake was not rescued in these larvae. This finding is consistent with the literature which demonstrate that glial derived ILPs do not control overall larval growth (Sousa-nunes et al., 2011).

4.3 *Ins/TOR signaling in the fat body of RanBPM mutants*

To determine which components of the InS and TOR pathways are disrupted in *RanBPM* mutants, we asked whether overexpression of downstream effector kinases *AKT* and *S6K* is capable of modifying *RanBPM* mutant phenotypes. When *AKT* was overexpressed in *RanBPM* mutants using *Lsp2*-GAL4 dye accumulation in the gut was significantly higher than the mutant controls (Figure 8A). Additionally the CNS size and the proliferation phenotype of the *RanBPM* mutant larvae were partially restored when AKT was overexpressed using LSP2- GAL4. Level of DILP2 in the IPCs of the *RanBPM* mutants expressing AKT was found to be reduced in comparison to the mutant control.

When *ppl*-GAL4 was used to drive UAS- *AKT* reporter in *RanBPM* mutants the expression did not reach the required threshold to induce a change in the feeding behavior. The level of accumulation in the gut observed when *AKT* was overexpressed under the control of *ppl*-GAL4 versus *Lsp2*-GAL4 can be explained in part by the mosaic pattern of expression exhibited by *ppl* (Bi et al., 2012), whereas *Lsp2* is expressed in all cells of the fat body. These results suggest that *RanBPM* phenotypes maybe due at least in part to reduced AKT function in the fat body.

Overexpression of S6K in the fat body showed an increase in the labelling of the phospho-H3 in the ventral nerve cord of the CNS compared to *RanBPM* homozygous mutants. However, the increased level of proliferation was not comparable to the CNS of the WT larvae. S6K overexpression led to an increase in the size of the CNS in *RanBPM* mutants. However the growth increase of the CNS did not reach the size of WT larval brain. Additionally TOR kinase, which is known to regulate its downstream targets S6K and 4E-BP, was also up-regulated in the fat body of the *RanBPM* mutants to determine its effects on brain growth. Overexpression of TOR kinase partially restored the cell proliferation in the CNS. Feeding behaviour of the larvae overexpressing TOR signaling proteins remain to be observed to better understand the role of TOR/S6K signaling in *RanBPM* mutant phenotypes.

In *Drosophila*, the fat body is a key organ in coupling the nutritional signal to the brain IPCs by a TOR- dependent mechanism. Studies have shown that TOR signaling is the major signaling pathway in the fat cells and not the PI3K pathway (Colombani et

al.,2003; Geminard et al., 2009). Studies from Pierre Leopold's laboratory has shown that although inhibition of InS/PI3K activity in the fat body led to a pronounced reduction of the fat body cells, it did not result in a delayed eclosion or a reduction in the overall size of the adult fly. Furthermore, inhibition of PI3K activity in fat cells was not found to influence DILP secretion from the brain (Geminard et al., 2009). In addition to these studies, Gould et al. found that removal of insulin receptor does not affect neuroblast growth or proliferation regardless of the nutrition conditions. Whereas the removal of the downstream components (ie. PI3K, Pdk1 and AKT) had profound effects on brain growth as suggested in part due to the function of Jeb/Alk signaling (Cheng et al., 2011). My own finding that up-regulation of *InR* in the fat body is not sufficient for starvation induced feeding behaviour is consistent with these reports suggesting that insulin signaling does not play an important role in the nutrient sensing mechanism for the non-autonomous regulation of the feeding behaviour.

The larval fat body organ is an important source of nutrients that get stored during the larval feeding stages of development. The fat body is sensitive to changes in nutrient conditions and therefore prolonged period of starvation or developmental processes (ie. metamorphosis) can trigger autophagy. Autophagy is a cellular response important for mobilizing nutrients to the developing tissues. To check whether autophagy can be induced in *RanBPM* mutants upon starvation Lyso Tracker dye was used to label autophagosomes in the dissected fat body organ. Punctate staining of Lyso Tracker red in *RanBPM* mutants was observed under nutrient deprived conditions. This

suggests that the fat body of *RanBPM* mutants responds properly to starvation by inducing autophagy. Although Lyso Tracker is considered as a reliable marker to trace autophagy, localization of *GFP-Atg8* can also be used as a more specific marker to label autophagosomal membranes. As discussed earlier, in response to starvation *TOR* signaling is inhibited thus inducing autophagy. Autophagy can also be triggered by directly inhibiting *TOR* via use of the drug, Rapamycin. Further experiments can be performed in *RanBPM* mutants using Rapamycin to evaluate the response of TOR signaling in the fat body. As a consequence of nutrient deprivation (ie. amino acids) the *Drosophila* fat body exhibits lipid aggregation as a way of remobilizing the nutrient stores. Consistently, lipid aggregation in the fat body was observed in the *RanBPM* mutants as a result of starvation. This finding suggest that in *RanBPM* mutants vesicle fusion is initiated in response to starvation indicating that the nutrient sensor mechanism of the fat body is perhaps not disrupted.

Conclusion

Taken together, findings from this report suggest a complex requirement for *RanBPM* in non-overlapping domains of expression involved in the systemic regulation of larval homeostasis and development. Our results suggest a role for *RanBPM* in the fat body for the proper expression and secretion of *DILP2*, neural stem cell proliferation, feeding behaviour and for the growth of the organism. My findings also suggest that *DILP6* secretion from the glial cells in the *RanBPM* mutants is sufficient to rescue the CNS proliferation phenotype.

Further experiments were conducted to determine which components of the InS and TOR pathways were disrupted in *RanBPM* mutants. To that extent, we asked whether overexpression of downstream effector kinases (i.e *AKT* and *S6K*) are capable of modifying *RanBPM* mutant phenotypes. Targeted expression of *AKT* in the fat body of the *RanBPM* mutants under there regulation of *Lsp2*-GAL4 or *ppl-GAL4* partially rescued the CNS proliferation phenotype. Reduced feeding and DILP2 retention phenotypes were also rescued in these larvae when *AKT* was overexpressed under the regulation of *Lsp2*-GAL4. These observations suggest that perhaps the *RanBPM* phenotypes maybe due at least in part to reduced *AKT* function in the fat body. Overexpression of *S6K* in the fat body of the *RanBPM* mutants under the control of either *Lsp2*-GAL4 or *ppl*-GAL4 showed an increase in the labelling of the phospho-H3 and the size of the CNS in comparison to RanBPM mutants. The growth deficit in these larvae was also rescued. Targeted expression of *TOR* in the fat body of the *RanBPM* mutants under the regulation

of *Lsp2*-GAL4 also showed an increase in the phospho-H3 labeling of the CNS in comparison to *RanBPM* mutants. Feeding experiments for the up regulation of *TOR* and *S6K* are yet to be performed and would provide insight into the role of TOR signaling in regulating RanBPM mutant phenotypes.

Results presented in this report together with previously published studies (Zhao and Campos, 2012) suggest that *dRanBPM,* a pleiotropic gene is required for proper insulin signaling in the *Drosophila* larva. Results reported here suggest a role for *RanBPM* in the fat body for the regulation of non-autonomous control of insulin secretion and feeding behaviour. Genetic epistasis experiments performed using *InS* and *TOR* components suggest a role of *AKT* in *RanBPM* mutant phenotypes for the fat body dependent remote control of DILP secretion. Additional studies are required to investigate the role of *TOR*/*S6K* signaling in the fat body for the regulation of feeding and DILP2 accumulation phenotypes of the *RanBPM* mutants.

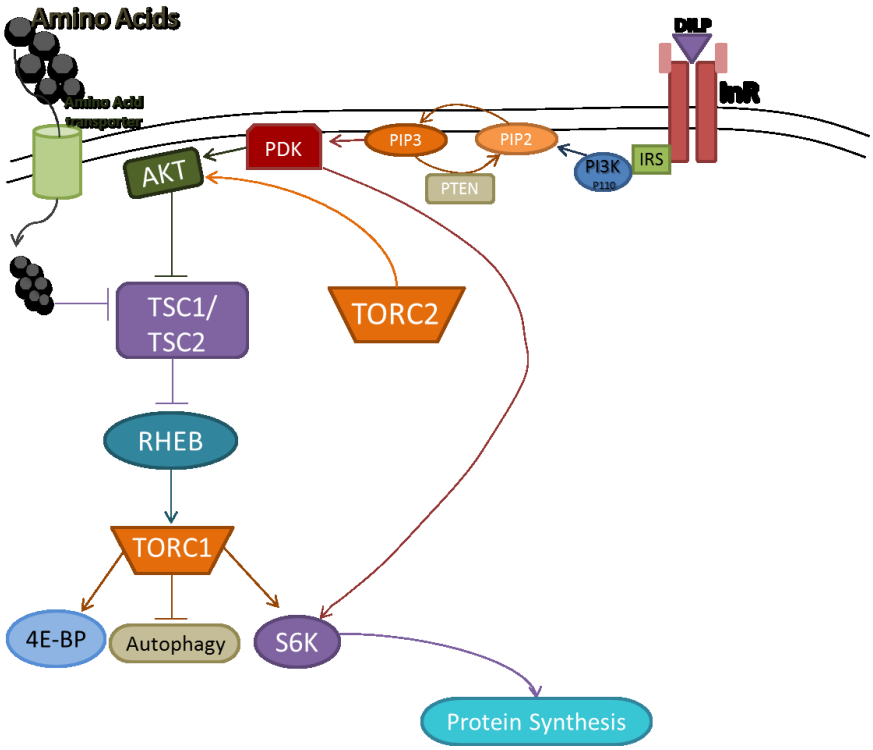

Figure 1. Ins/TOR signalling. *Drosophila* insulin like peptide (DILP) binds and activates the insulin receptor (InR). Insulin signalling is mediated through the InR upon binding of the insulin receptor substrate (IRS). This leads to the activation of phosphoinositide-3-kinase (PI3K) which converts phosphatidylinositol 3,4-biphosphate 2 (PIP2) to PIP3. PIP3 stimulates PDK (phosphoinositide-dependent kinase) and activates serine/threonine

protein kinase Akt1 (also called PKB; protein kinase B). The phosphatase and tensin homologue (PTEN) phosphatase antagonizes the activity of PI3K by reverting PIP3 back to PIP2. PKB inhibits tuberous sclerosis 1 (TSC1/TSC2) complex and TSC1/TSC2 inhibits RAS homologue enriched in brain (RHEB). Downstream effectors of TOR include S6 kinase and initiation factor 4E-binding protein (4e-BP). TOR kinase activates S6K and inhibits the negative regulator 4E-BP to stimulate translation. In addition, TOR is involved in regulating catabolic processes such as autophagy (Reviewed by Oldham and Hafen, 2003)

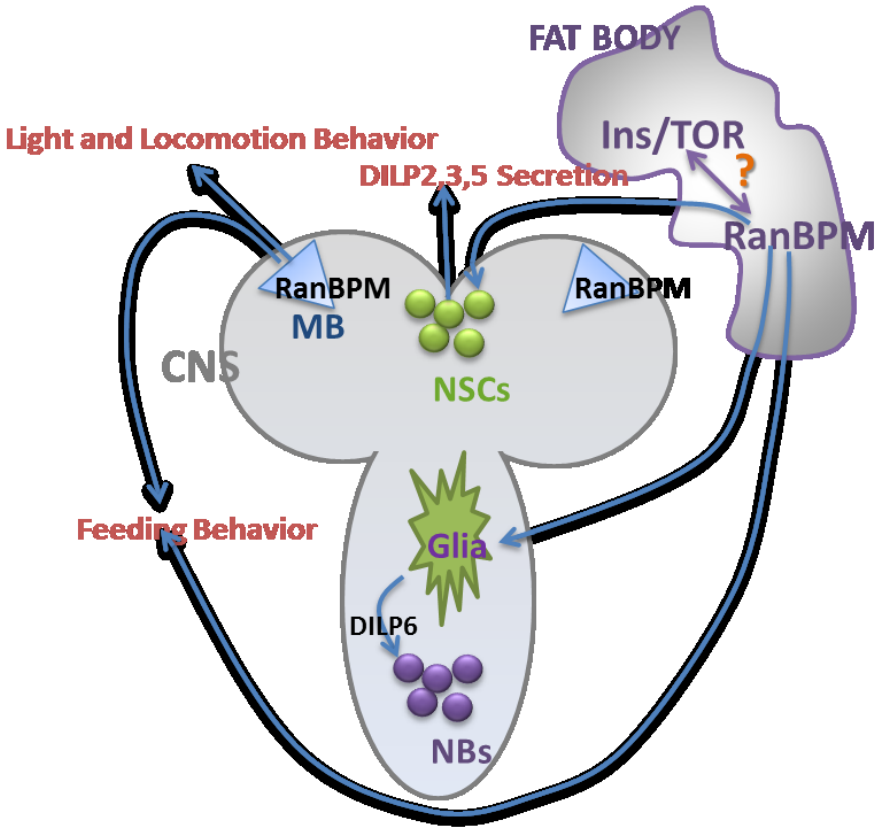

Figure 2. Schematic representation of the proposed model for *RanBPM* function. Recent evidence has suggested a role for RanBPM in the fat body in controlling the starvation induced food intake, growth, CNS proliferation and insulin secretion. Role for RanBPM in regulating larval feeding behaviour, light and locomotion behaviour through the mushroom body (MB) function has been previously identified (Scantelbury 2010). Recent evidence suggests a role for RanBPM in the fat body for the regulation of feeding behaviour, growth, neuroblast (NBs) proliferation and insulin secretion from the neurosecretory cells (NSCs) of the CNS. Schematic also represents the reactivation of neuroblast cells via the local release of dILP6 from the glial cells of the CNS. My current work is focused on analyzing the role of Ins/TOR signalling in the fat body of *Drosophila RanBPM* mutants for modulating the remote control of insulin secretion and feeding behavior.

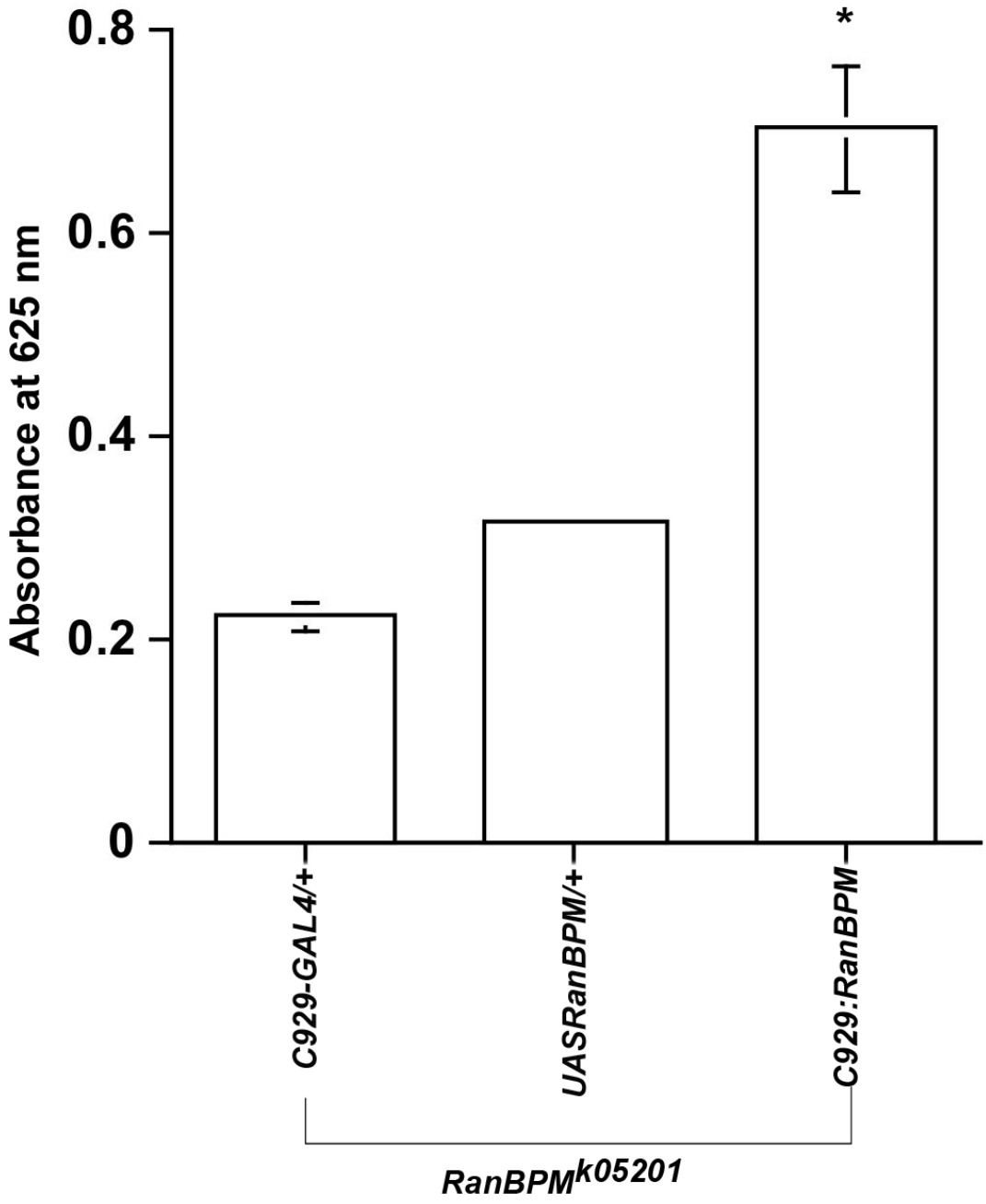

Figure 3. Targeted expression of *RanBPM* in neurosecretory cells is sufficient to rescue the feeding phenotype of *RanBPM* mutants. The graph depicts the absorbance at 625nm (A665nm) of larval extracts as a measure of the amount of food present in the

gut. Targeted expression of neurosecretory cells was achieved by using *C929-GAL4* element to regulate the expression of a *UAS- RanBPM* construct in *RanBPM* mutant background (*RanBPM*^{k05201}*; C929: RanBPM*^{k05201}). Targeted expression of *RanBPM* in neurosecretory cells caused a significant increase in the food intake of *RanBPM* mutants (*RanBPM*^{K05201} ;*C929:RanBPM*) relative to that of mutants carrying the GAL4 (*RanBPM*^{k05201}*; C929-GAL4/+*) or the UAS construct alone (*RanBPM*^{k05201}*; UAS-RanBPM/+)*. The amount of food present in *RanBPM*^{k05201}*; C929: RanBPM*^{k05201} is not significantly different from that of controls (*y,w*). All measurements are shown as mean values and +/- SEM. (N ≥ 3 (180 third instar larvae), ANOVA $F(3,12) = 112.8$, $p \leq 0.000$).

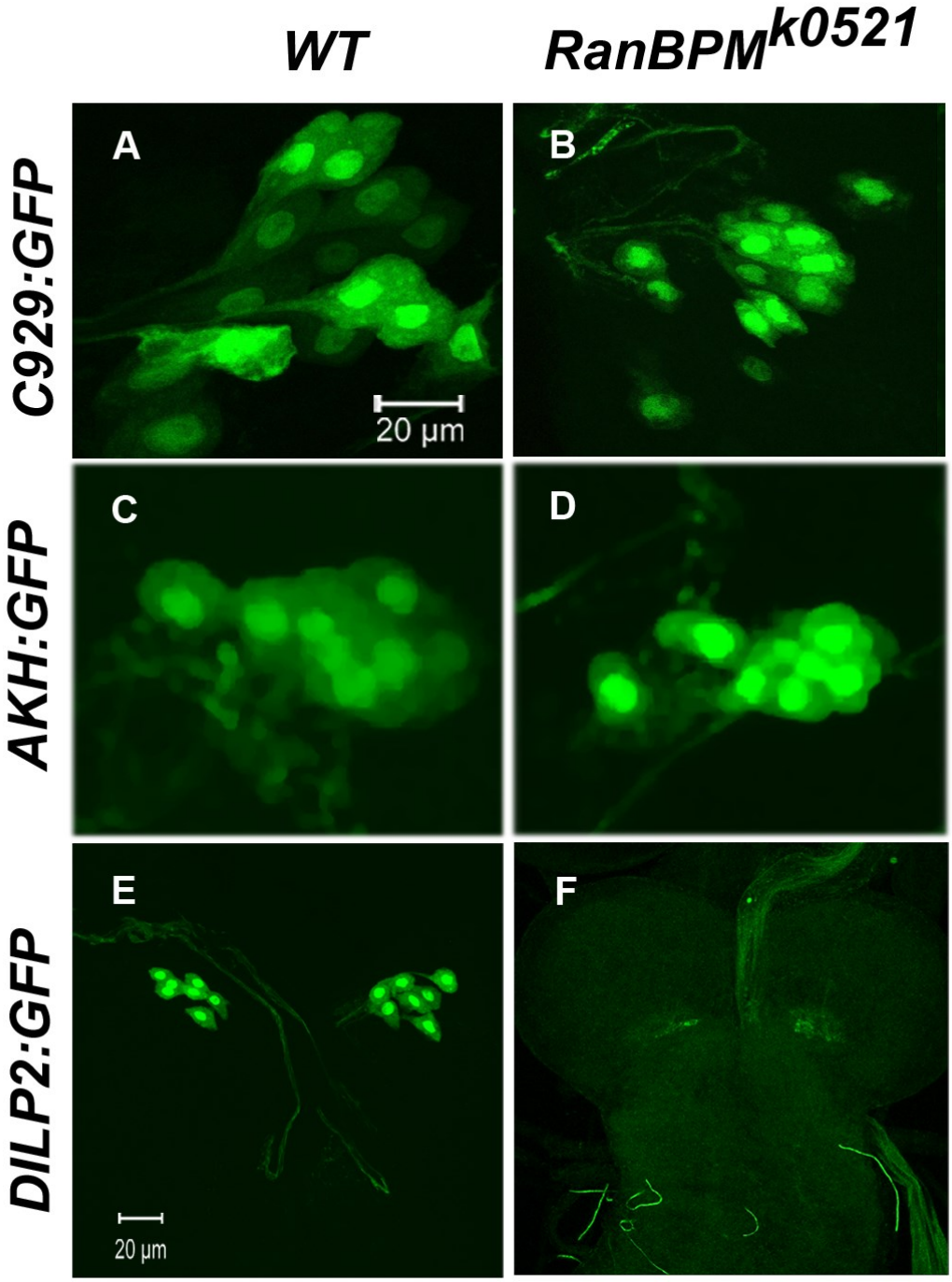

Figure 4. Impact of *RanBPM* mutations on subsets of neurosecretory cells. Expression of a nuclear GFP construct (*UAS-GFP:LacZ.nls*) regulated by the *C929-GAL4* (**A** and **B**),

AKH-GAL4 (**C** and **D**) and *DILP-2-GAL4* (**E** and **F**) was used to visualize the median neurosecretory cells cluster (mNSC) , the AKH (adipokinetic hormone) producing cells in the ring gland and the DILP2- producing subset of the mNSC respectively in wild type (WT) and *RanBPM* mutants (*RanBPM*^{K0521}).While the number and position of AKH cells did not differ in mutant and wild type specimens (**C** and **D**) the mNSC cluster was consistently smaller in *RanBPM* mutants (**A** and **B** see Additional file 4). In contrast, the *DILP2* reporter is not expressed in *RanBPM* mutant brains (**E** and **F**). Scale bar in **A** valid for **B** and **C**. Scale bar in **E** valid for **F.**

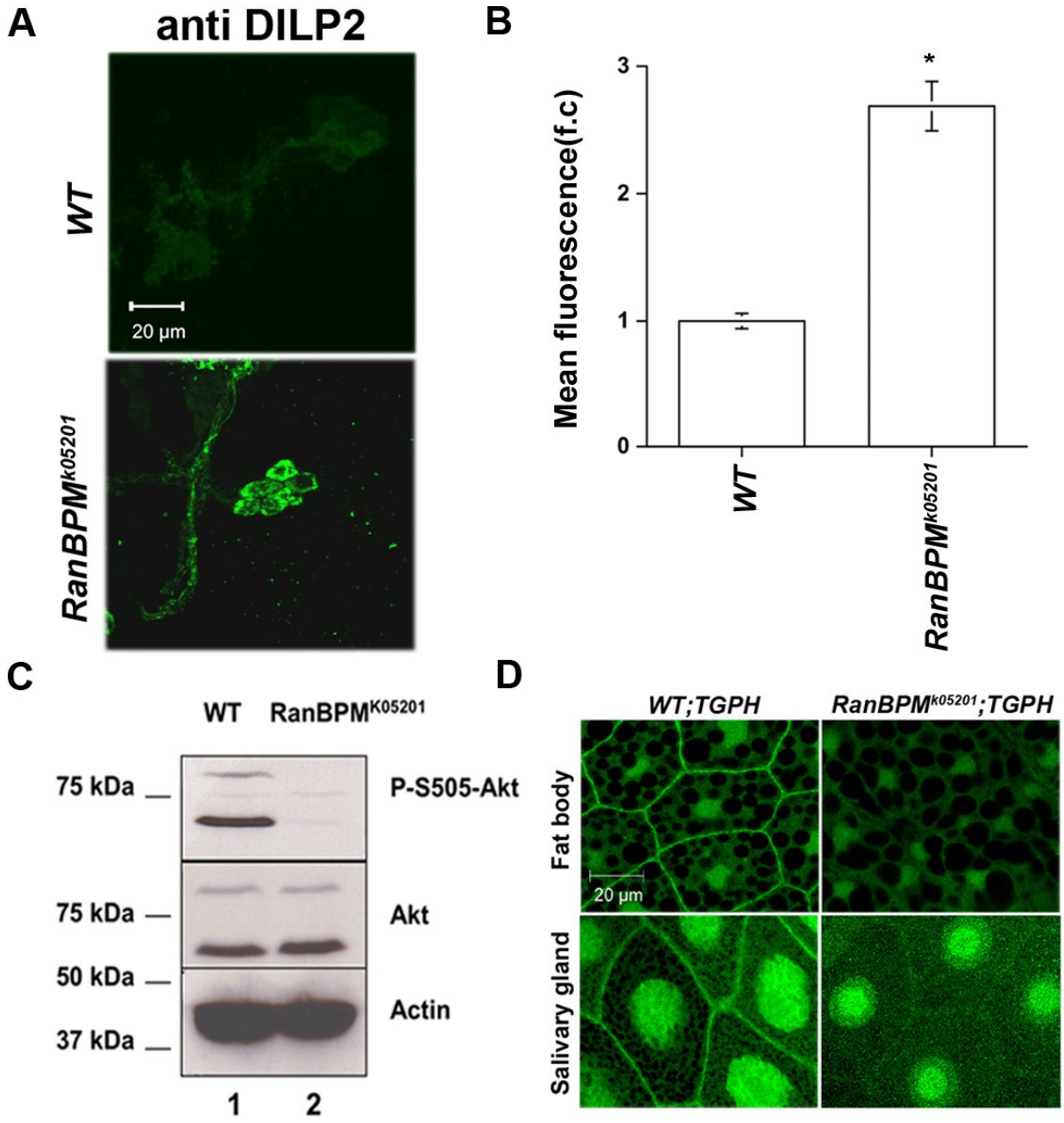

Figure 5. *RanBPM* mutant phenotypes consistent with disrupted systemic insulin signaling. **A**- Representative photomicrographs of dissected brains from wild type (WT) and *RanBPM* mutants (*RanBPM*^{K05201}) immunolabeled with anti-DILP2 antibodies and

imaged by confocal microscopy using identical laser and scan settings. Images represent Z-stacks of 8-12 sections at 1µm intervals. Scale bar valid for both panels **B-**The graph depicts the fluorescence intensity across the insulin producing cell clusters of wild type and *RanBPM* mutant larvae. ($N \geq 28$ for each genotype, Student's T- test $*p \leq 0.001$). **C-** Representative Western blot showing a marked decrease in the level of activated phospho-AKT (pAKT) in *RanBPM* mutant larval extracts relative to WT control. In contrast total AKT is not affected by lack of *RanBPM* gene function. Actin is shown as a control for sample loading. Quantitation relative to the internal actin control is shown in Additional file 5**. D-** Representative confocal micrographs of larval fat bodies and salivary glands from WT and *RanBPM* mutants carrying the TGPH construct to detect InR/PI3K activity. The characteristic accumulation of the GPH fusion protein in the plasma membrane of either tissue is markedly reduced in the *RanBPM* mutant larvae.

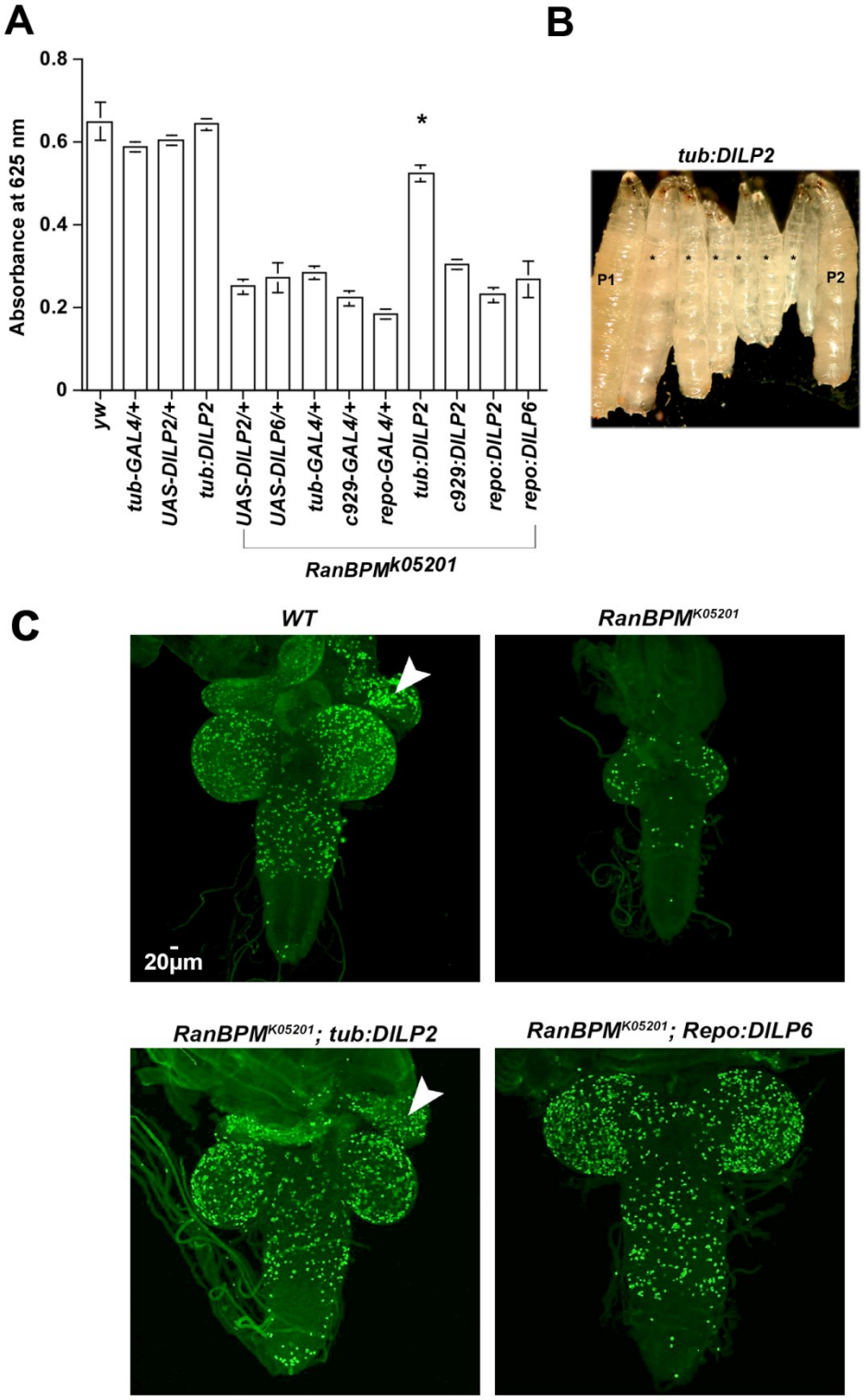
A
B
Absorbance at 625 nm
0.8
0.6
0.4
0.2
0
*
yw
tub-GAL4/+
UAS-DILP2/+
tub:DILP2
UAS-DILP2/+
UAS-DILP6/+
tub-GAL4/+
c929-GAL4/+
repo-GAL4/+
tub:DILP2
c929:DILP2
repo:DILP2
repo:DILP6
RanBPMk05201
tub:DILP2
P1
P2
C
WT
RanBPMK05201
20µm
RanBPMK05201; tub:DILP2
RanBPMK05201; Repo:DILP6

Figure 6. Ubiquitous expression of *DILP2* partially restores *RanBPM* mutant phenotype

A- The graph depicts the absorbance at 625nm (A625nm) of larval extracts as a measure of the amount of food present in the gut. Over expression of *dILP2* under the control of the ubiquitous GAL4 driver *tub-GAL4* (*RanBPM* ^{K05201}; *tub: dILP2*) significantly increased A625nm relative to that of mutants carrying only the GAL4 (*RanBPM*^{k05201}*; tub-GAL4/+*) or the UAS construct (*RanBPM*^{k05201}*; UAS-RanBPM/+).* Over expression of *dILP2* in a wild type background (*tub:dILP2)* did not significantly increase A625nm of larval extracts. All measurements are shown as mean values and +/- SEM (N ≥ 3 (180 larvae, ANOVA F(12,50) = 109.99, *P≤0.001). **B**- Representative micrographs of *RanBPM* ^{K05201}*; tub: dILP2* (*) larvae flanked by parental controls (**P1**, *RanBPM* ^{K05201}/ +; *tub-GAL4* and **P2**, *RanBPM* ^{K0520} / + ; *UAS dILP2*) and homozygous *RanBPM* ^{K05201} (**m**). **C-** Representative confocal micrographs of dissected larval brains immunolabeled with anti-phospho H3 antibody to detect mitotically-active cells. Images shown are projected Z-series collected at 2 µm intervals from 24-33 sections of wild type (WT), 14-17 sections of homozygous *RanBPM* ^{K05201} , 18-25 sections of *RanBPM* ^{K05201}*;tub:DILP2* and 16-23 sections of *RanBPM* ^{K05201}*;repo:DILP6*. Lack of *RanBPM* function markedly reduces proliferation in the CNS. The eye-antennal imaginal disc is rarely visible in the third instar *RanBPM* ^{K05201}mutant specimens (arrowhead in WT). *RanBPM* mutant larva in which *DILP2* was ubiquitously expressed under the regulation of the tubulin (tub) promoter (*RanBPM* ^{K05201}*;tub:DILP2*) is larger, displays increased phospho H3 labelling when compared to homozygous *RanBPM* ^{K05201} mutant and is indistinguishable from WT control. The eye

antennal imaginal disc of *RanBPM* ^{K05201}*;tub:DILP2* is visible and labelled by phospho H3 antibody (arrowhead). Targeted expression of *DILP6* under the regulation of a pan-glial driver *repo-GAL4* is sufficient to restore proliferation and growth in the nervous system but not in the eye imaginal discs of *RanBPM* mutants (*RanBPM* ^{K05201}*; repo:DILP2*). Scale bar is valid for all panels in **C**.

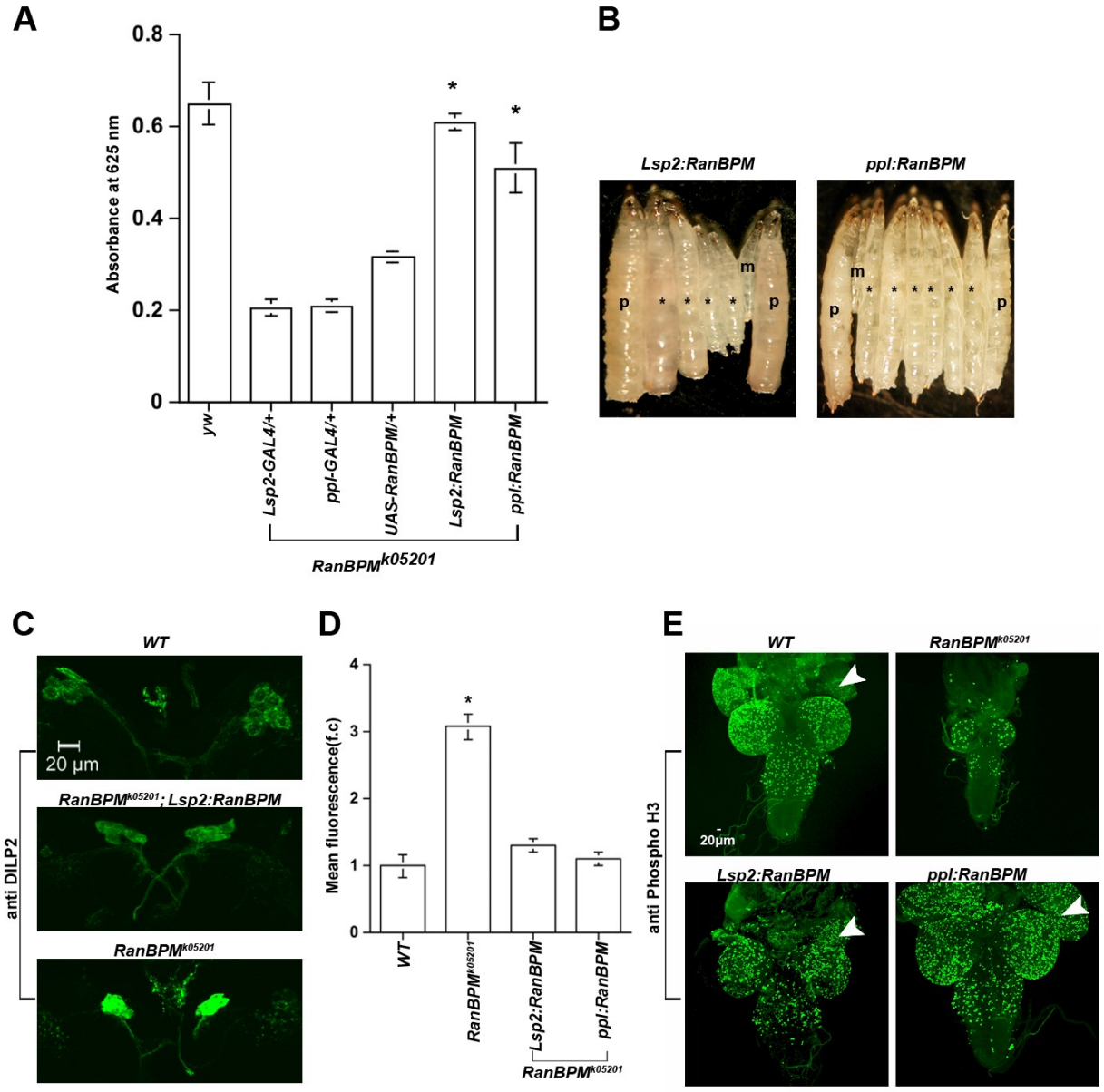

Figure 7. Targeted expression in the fat body rescues *RanBPM* mutant phenotype. **A-** The graph depicts the absorbance at 625nm (A625nm) of larval extracts as a measure of the amount of food present in the gut. Expression of *RanBPM* in the fat body using two independent GAL4 drivers expressed in this organ significantly increased the A625nm of extracts obtained from homozygous *RanBPM* mutant larvae (**RanBPM* ^{K05201}*; Lsp2:RanBPM* and *RanBPM* ^{K05201}*; ppl:RanBPM)* above that of mutants carrying the GAL4 (*RanBPM* ^{K05201}; *Lsp2 (or ppl)-GAL4/+*) or the UAS construct (*RanBPM* ^{K0520}; *UAS-RanBPM*/+) only, but it is not significantly different from that for parental control strain (*y,w*). All measurements are shown as mean values and +/- SEM (N ≥3 (180 larvae), ANOVA F(5,20) = 138.67, p≤0.001). **B**- Representative micrographs of *RanBPM* ^{K05201}*; Lsp2 (or ppl): RanBPM* (*) larvae flanked by parental controls (**P1**, *RanBPM* ^{K05201}/ +; *Lsp2 (*or *ppl)-GAL4* and **P2**, *RanBPM* ^{K0520} / + ; *UAS-RanBPM*) and homozygous *RanBPM* ^{K05201} mutant larvae (**m**). **C-.** Representative photomicrographs of larval brains dissected from wild type (WT), *RanBPM* mutant (*RanBPM*^{K05201}) and *RanBPM* mutants expressing *RanBPM* in the fat body under the regulation of the *Lsp2-GAL driver* (*RanBPM*^{K05201}*; Lsp2:RanBPM*) immune stained with anti-DILP2 antibodies and imaged by confocal microscopy using identical laser and scan settings. Images represent Z-stacks projections of 8-14 sections at 1 µm intervals. **D**- The graph depicts the fluorescence intensity across the insulin producing cell clusters for the genotypes shown in C and for *RanBPM*^{K05201}*; ppl:RanBPM*. (N ≥ 24 for each genotype, ANOVA F(2,80)=37.83, P≤0.000).

Scale bar valid for all photomicrographs in this panel. **E-**Representative confocal micrographs of larval brains immunolabeled with anti-phospho H3 antibody to detect mitotically-active cells. Images shown are projected Z-series obtained from 18-26 sections of wild type, *16-25* sections of *RanBPM* ^{K05201}*;Lsp2 (*or *ppl):RanBPM* , and *14-20* sections of *RanBPM* ^{K05201}. All Z series were obtained at 2 µm intervals. Lack of *RanBPM* function markedly reduces proliferation in the CNS and the eye-antennal imaginal disc is rarely visible (*RanBPM* ^{K05201}). The CNS dissected from *RanBPM* mutant larva expressing *RanBPM* in the fat body is generally larger, displays increased phospho H3 labelling in the CNS and eye imaginal disc (*RanBPM* ^{K05201}*;Lsp2 (*or *ppl):RanBPM*). Arrowhead points to eye imaginal disc. Scale bar is valid for all photomicrographs in this panel.

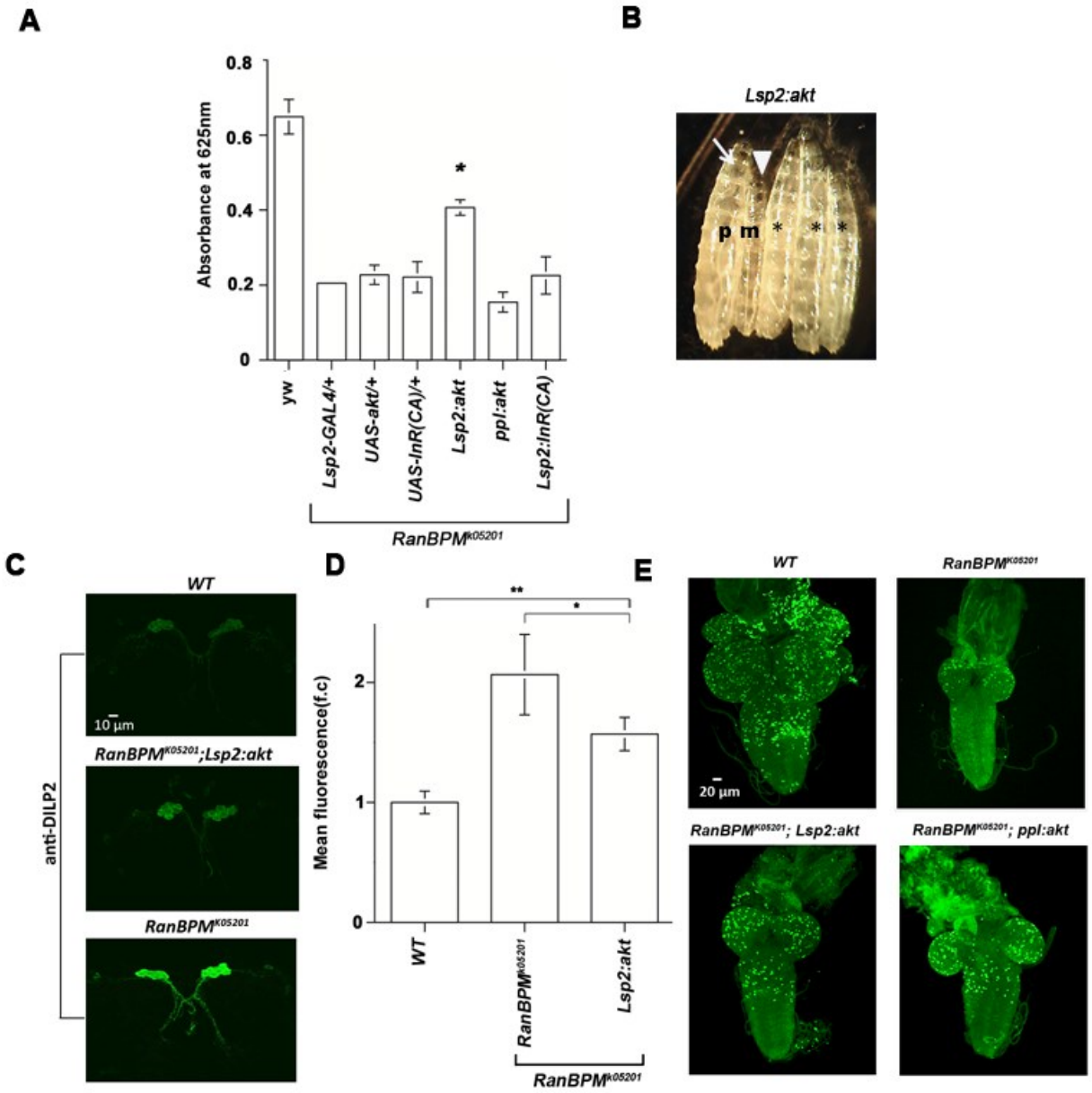

Figure 8. Up- regulation of *AKT* in the fat body partially rescues *RanBPM* mutant phenotypes A- The graph depicts the absorbance at 625nm (A625nm) of larval extracts as a measure of the amount of food present in the gut. Up-regulation of *AKT* in the fat body using *Lsp2*-GAL4 significantly increased the A625nm of extracts obtained from

homozygous *RanBPM* mutant larvae (**AKT*; *RanBPM* ^{K05201}*; Lsp2*) above that of mutants carrying the GAL4 (*RanBPM* ^{K05201}; *Lsp2-GAL4/+*) or the UAS construct (*UAS-AKT; RanBPM* ^{K0520}). Expression of *AKT* using *ppl*-GAL4 was not sufficient to increase the A625nm of larval extracts (*AKT*;*RanBPM* ^{K05201}*; ppl).* Targeted expression of *InR(CA)* using *Lsp2*-GAL4 (*RanBPM* ^{K05201}*; Lsp2: InR (CA)*) did not increase the A625nm of the larval extracts above that of the mutants carrying the GAL4 (*RanBPM* ^{K05201}; *Lsp2-GAL4/+*) or the UAS constructs (*RanBPM* ^{K05201}; *UAS-InR(CA)/+*). All measurements are shown as mean values and +/- SEM (N ≥3 (180 larvae), ANOVA F(6,18) = 25.33, p≤0.000). **B**- Representative micrographs of *AKT*: *RanBPM* ^{K05201}*; Lsp2* (*) larvae next to the parental control (**P,** *RanBPM* ^{K05201}/ +; *Lsp2*) and homozygous *RanBPM* ^{K05201} mutant larvae (**m**). **C-** Representative photomicrographs of larval brains dissected from wild type (WT), *RanBPM* mutant (*RanBPM*^{K05201}) and *RanBPM* mutants expressing *AKT* in the fat body under the regulation of the *Lsp2-GAL4* driver or *ppl-GAL4*(*AKT; RanBPM*^{K05201}*; Lsp2* or *AKT; RanBPM*^{K05201}*;ppl*) immune stained with anti-DILP2 antibodies and imaged by confocal microscopy using identical laser and scan settings. Images represent Z-stacks projections of 8-14 sections at 1 µm intervals. **D**- The graph depicts the fluorescence intensity across the insulin producing cell clusters for the genotypes shown in C (N ≥ 15 for each genotype, ANOVA F(2,47)=17.57, P≤0.000). Scale bar valid for all photomicrographs in this panel. **E-** Representative confocal micrographs of larval brains immunolabeled with anti-phospho H3 antibody to detect mitotically-active cells. Images shown are projected Z-series obtained from 20-28 sections of wild type, *16-25* sections

of *AKT;RanBPM* ^{K05201}*;Lsp2 (*or *ppl)*, and *14-20* sections of *RanBPM* ^{K05201}. All Z series were obtained at 2 µm intervals. The CNS dissected from *RanBPM* mutant larva expressing *AKT* in the fat body display an increase in phospho H3 labelling in the CNS (*AKT*; *RanBPM* ^{K05201}*;Lsp2 (*or *ppl)*) compared to *RanBPM* mutant control.

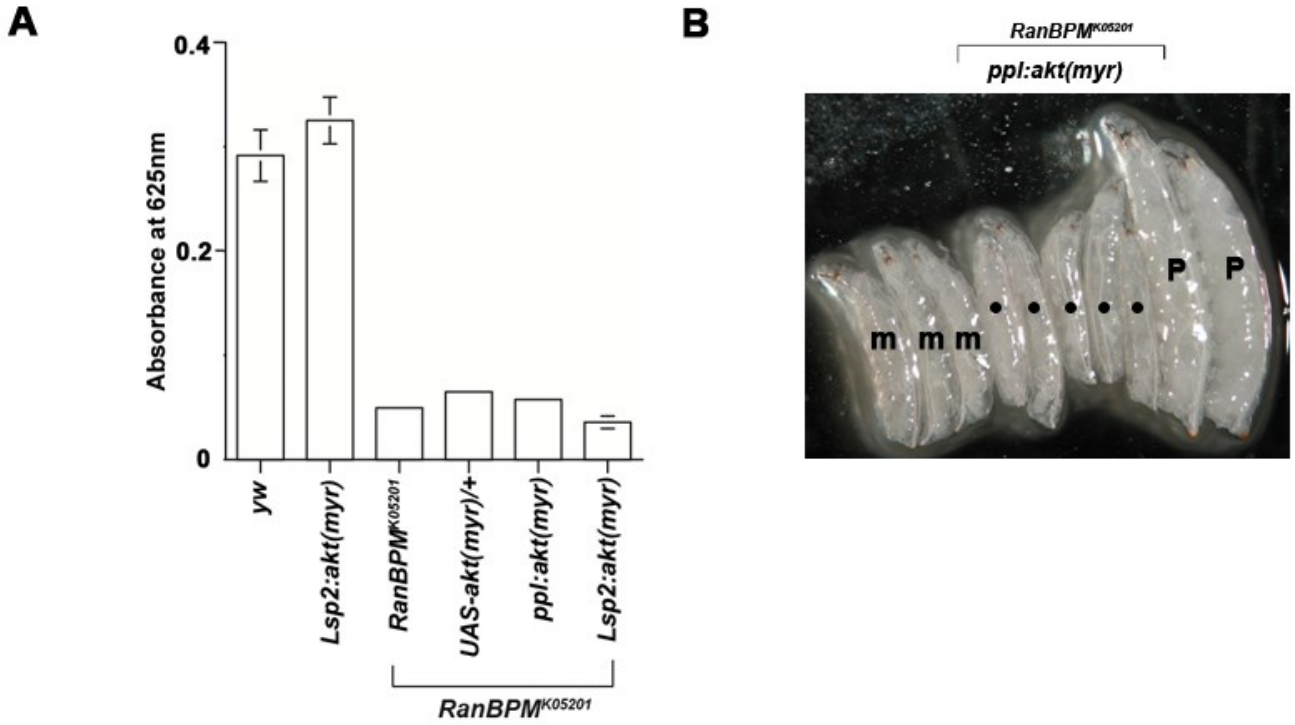

Figure 9. Targeted expression of *AKT (myr)* in the fat body of *RanBPM* mutants. A- The graph depicts the absorbance at 625nm (A625nm) of larval extracts. Up-regulation of *AKT(myr)* in the fat body using *Lsp2*-GAL4 or ppl-GAL4 is not sufficient to increase the A625nm of *RanBPM* mutant larval extracts (*RanBPM* ^{K05201}*; Lsp2: AKT(myr)*) compared to the mutants carrying the GAL4 (*RanBPM* ^{K05201}; *Lsp2-GAL4/+*) or the UAS construct (*RanBPM* ^{K05201}; *UAS-AKT(myr)*). All measurements are shown as mean values and +/-

SEM (N ≥2 (20 larvae), ANOVA F(5,17) = 277.23, p≤0.000). **B**- Representative micrographs of *RanBPM* ^{K05201}*; Lsp2:AKT(myr)* (*) larvae next to parental controls (**P,** *RanBPM* ^{K05201}/ +; *Lsp2*) and homozygous *RanBPM* ^{K05201} mutant larvae (**m**).

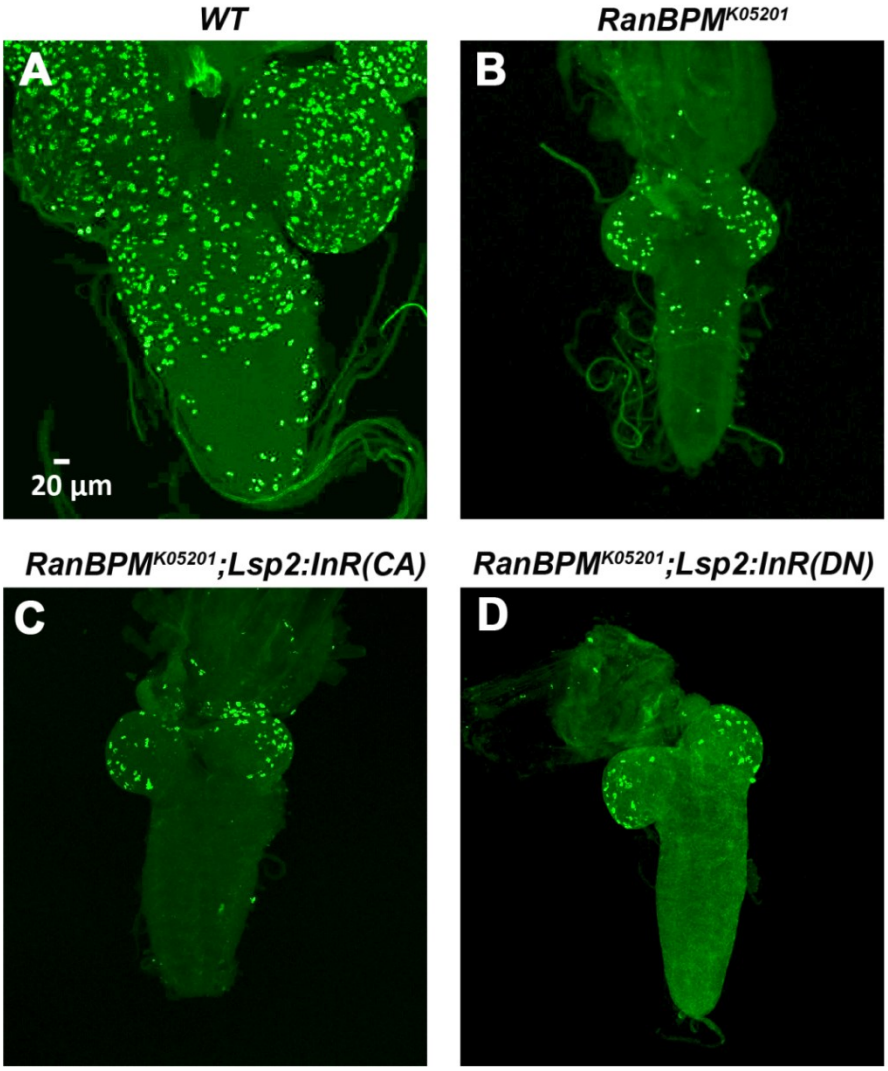

Figure 10. Expression of *InR* in the fat body of *RanBPM* mutants. Representative confocal micrographs of larval brains immunolabeled with anti-phospho H3 antibody to detect mitotically-active cells. Images shown are projected Z-series obtained from **A-**18-

25 sections of wild type, **B-***12-18* sections of *RanBPM* ^{K05201} **C-** *18-26* sections of *RanBPM*^{K05201}*; Lsp2-GAL4:UAS InR (CA),* and **D-***14-18* sections of *RanBPM*^{K05201}*; Lsp2-GAL4:UAS InR (DN)*. All Z series were obtained at 2 µm intervals. Up-regulation *(RanBPM*^{K05201}*; Lsp2-GAL4:UAS InR (CA))* or down-regulation (*RanBPM*^{K05201}*; Lsp2-GAL4:UAS InR (DN))* of insulin receptor did not increase the phospho-H3 labeling of the CNS compared to *RanBPM* mutant control.

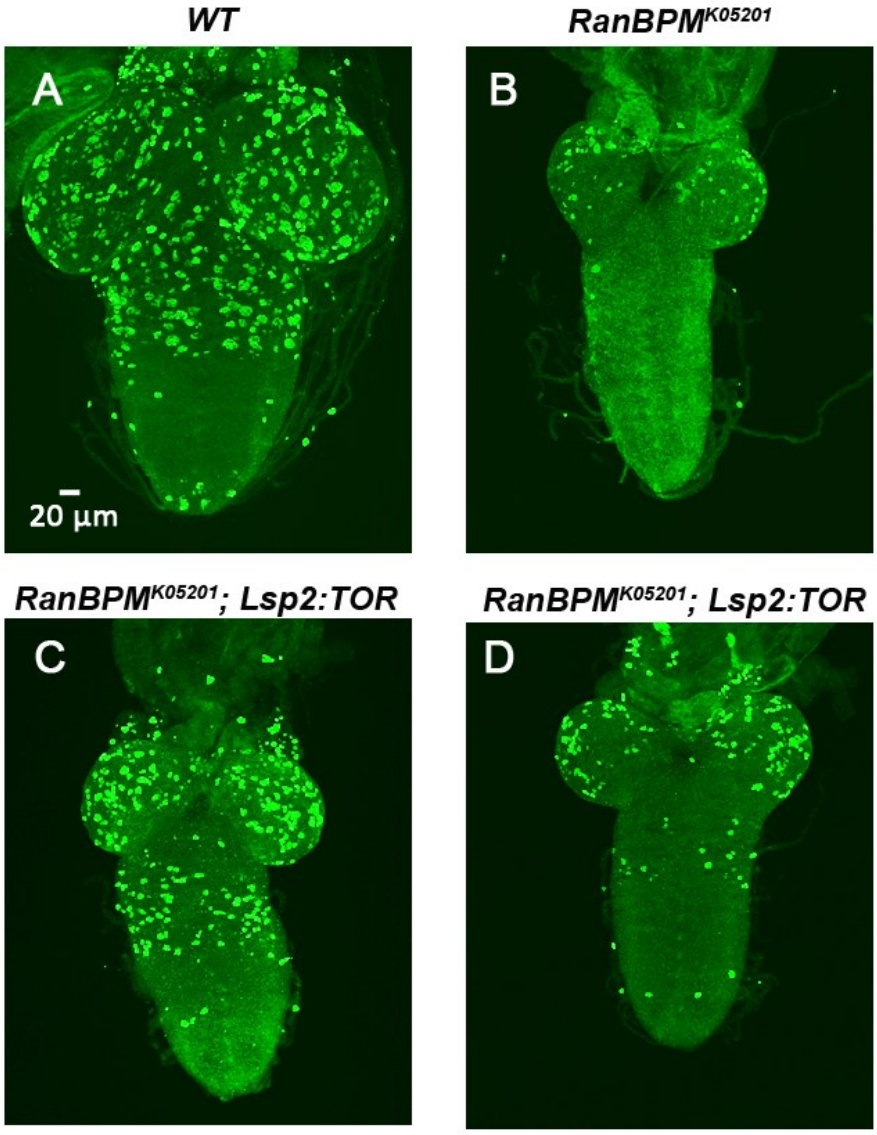

Figure 11. Targeted Expression of *TOR* in the fat body partially rescues the CNS proliferation of *RanBPM* mutants. Representative confocal micrographs of larval brains immunolabeled with anti-phospho H3 antibody. Images shown are projected Z-series obtained from **A-**18-26 sections of wild type, **B-***14-20* sections of *RanBPM K05201* and **C and D-***13-20* sections of *RanBPM*^{K05201}*; Lsp2-GAL4:UAS TOR* . All Z series were obtained

at 2 µm intervals. Overexpressing Target of Rapamycin (TOR) in the fat body under the regulation of **(C)** *Lsp2*-GAL4 in *RanBPM* mutants increased the phospho-H3 labeling of the CNS compared to the *RanBPM* mutant control. When *TOR* was overexpressed in the fat body under the regulation of *ppl*-GAL4 the phospho-H3 labeling of the CNS did not increase compare to the *RanBPM* mutant control. The size of the CNS did not appear to increase when *TOR* was up-regulated under the regulation of either *Lsp2*-GAL4 or *ppl*-GAL4.

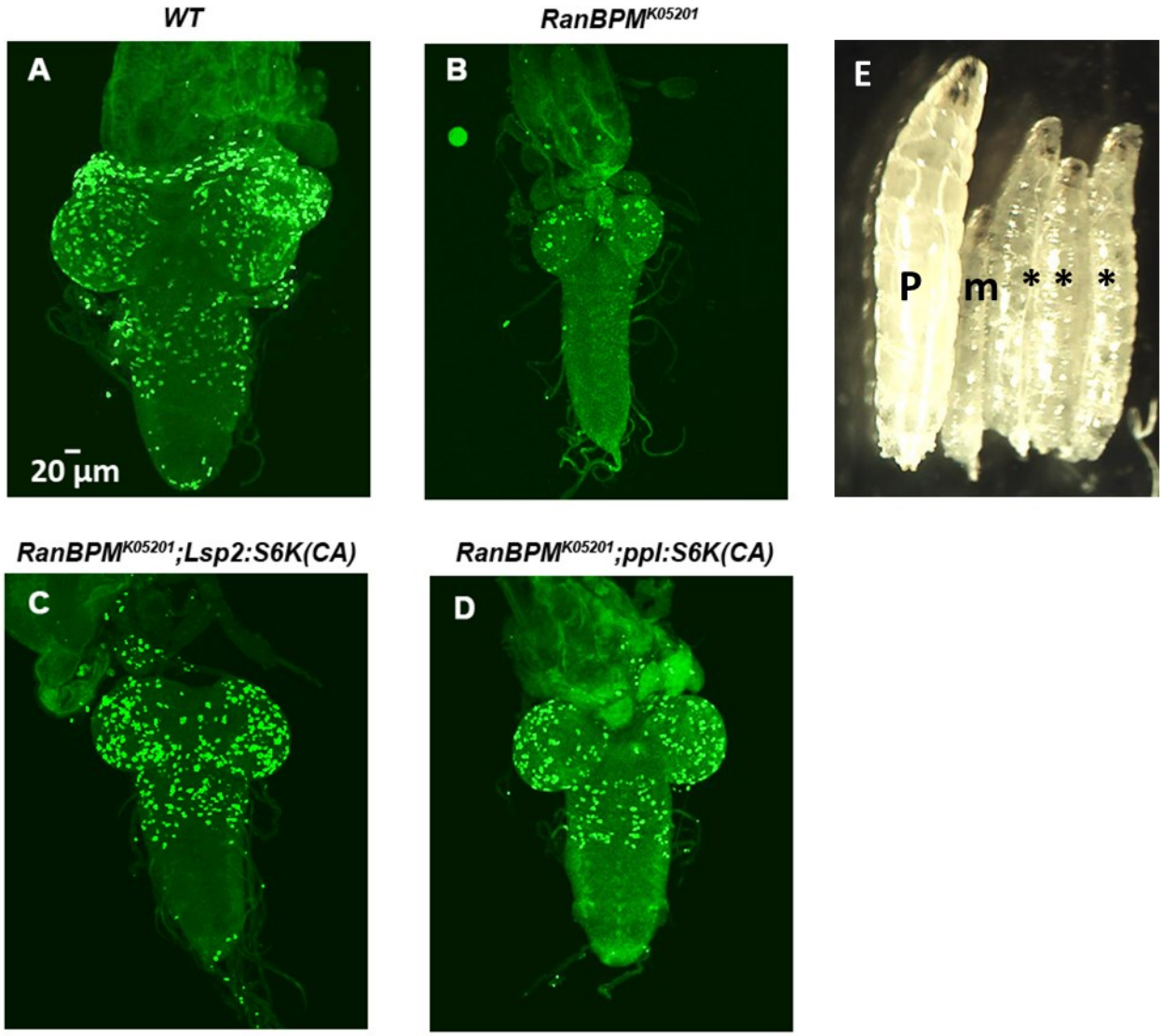

Figure 12. Over expression of *S6K* in the fat body partially rescues the CNS proliferation and the size of *RanBPM* mutants. Representative confocal micrographs of larval brains immunolabeled with anti-phospho H3 antibody. Images shown are projected Z-series obtained from **A-**18-26 sections of wild type, **B-***15-23* sections of *RanBPM* ^{K05201} and **C**

and D-*14-26* sections of *RanBPM*^{K05201}*; Lsp2-GAL4:UAS S6K* (or *ppl*-GAL4) . All Z series were obtained at 2 µm intervals. Up-regulation of S6K in the fat body under the regulation of *Lsp2*-GAL4 or *ppl*-GAL4 in *RanBPM* mutants increased the phospho-H3 labeling of the CNS compared to the *RanBPM* mutant control. The size of the CNS appeared bigger than the RanBPM mutant control when *S6K* was up-regulated under the regulation of either *Lsp2*-GAL4 or *ppl*-GAL4. **E**- Representative micrographs of *RanBPM* ^{K05201}*; Lsp2-GAL4*:*UAS S6K(CA)* (*) larvae next to the parental control (**P,** *RanBPM* ^{K05201}/ +; *Lsp2*) and homozygous *RanBPM* ^{K05201} mutant larvae (**m**).

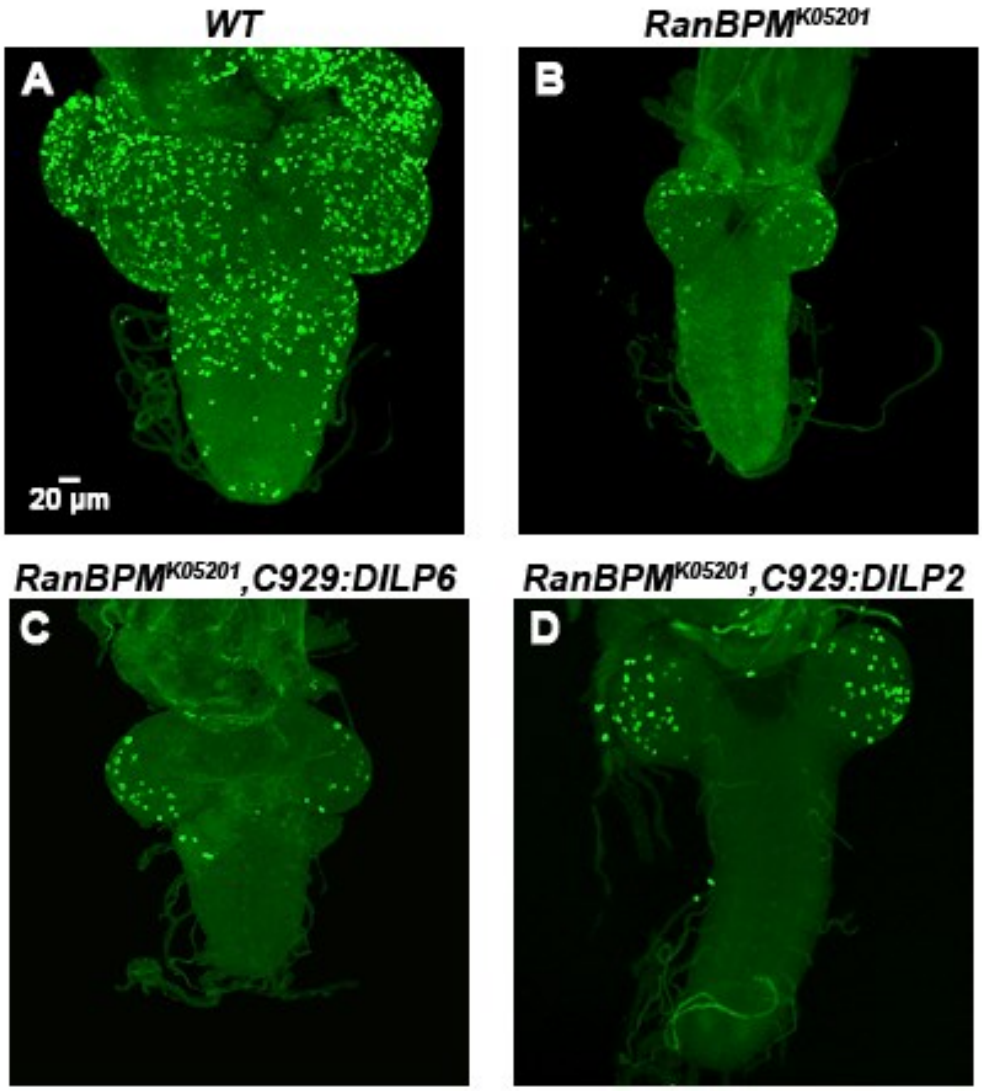

Figure 13. Targeted expression of dILPs in DIMM- positive peptidergic neurons in RanBPM mutants. Representative confocal micrographs of larval brains immunolabeled with anti-phospho H3 antibody. Images shown are projected Z-series obtained from **A-** 18-26 sections of wild type, **B-***14-20* sections of *RanBPM* ^{K05201} **C-** *10-15* sections of *C929-GAL4,RanBPM*^{K05201}*; UASDILP2* and **C-** *14-20* sections of *C929,GAL4,RanBPM*^{K05201}*; UASDILP6* . All Z series were obtained at 2 µm intervals. When either *DILP2* or *DILP6*

were overexpressed under the regulation of *C929-GAL4* phospho-H3 labeling appeared indistinguishable compared to RanBPM mutants and therefore CNS proliferation was not rescued.

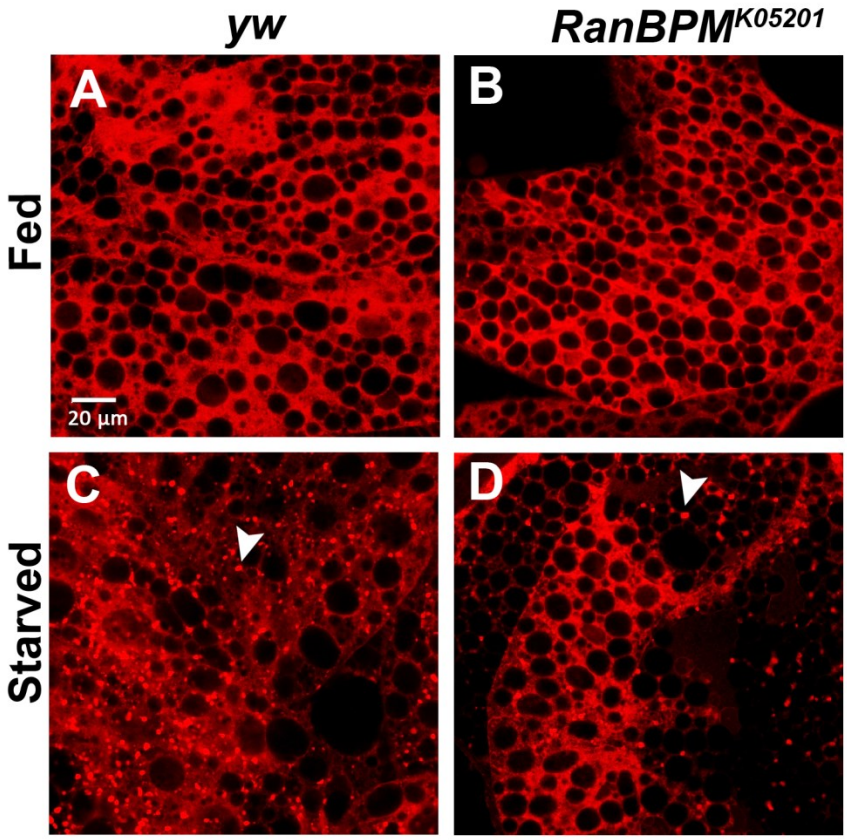

Figure 14. Examining autophagy in *RanBPM*^{K05201} mutants using LysoTracker probe. Representative confocal micrographs of larval fat body stained with LysoTracker Red DND-99 (Molecular Probes) to detect autophagosomes. Images shown are snapshots of **A**-wild type under fed conditions **B-** *RanBPM*^{K05201} mutants under fed conditions **C-** wild type under starved conditions and **D-** *RanBPM*^{K05201} mutants under starved conditions. Increased punctate staining (indicated by the arrow heads) of LysoTracker probe was

detected under starved conditions in the fat body of both the *RanBPM*^{K05201} mutants and wild type larvae.

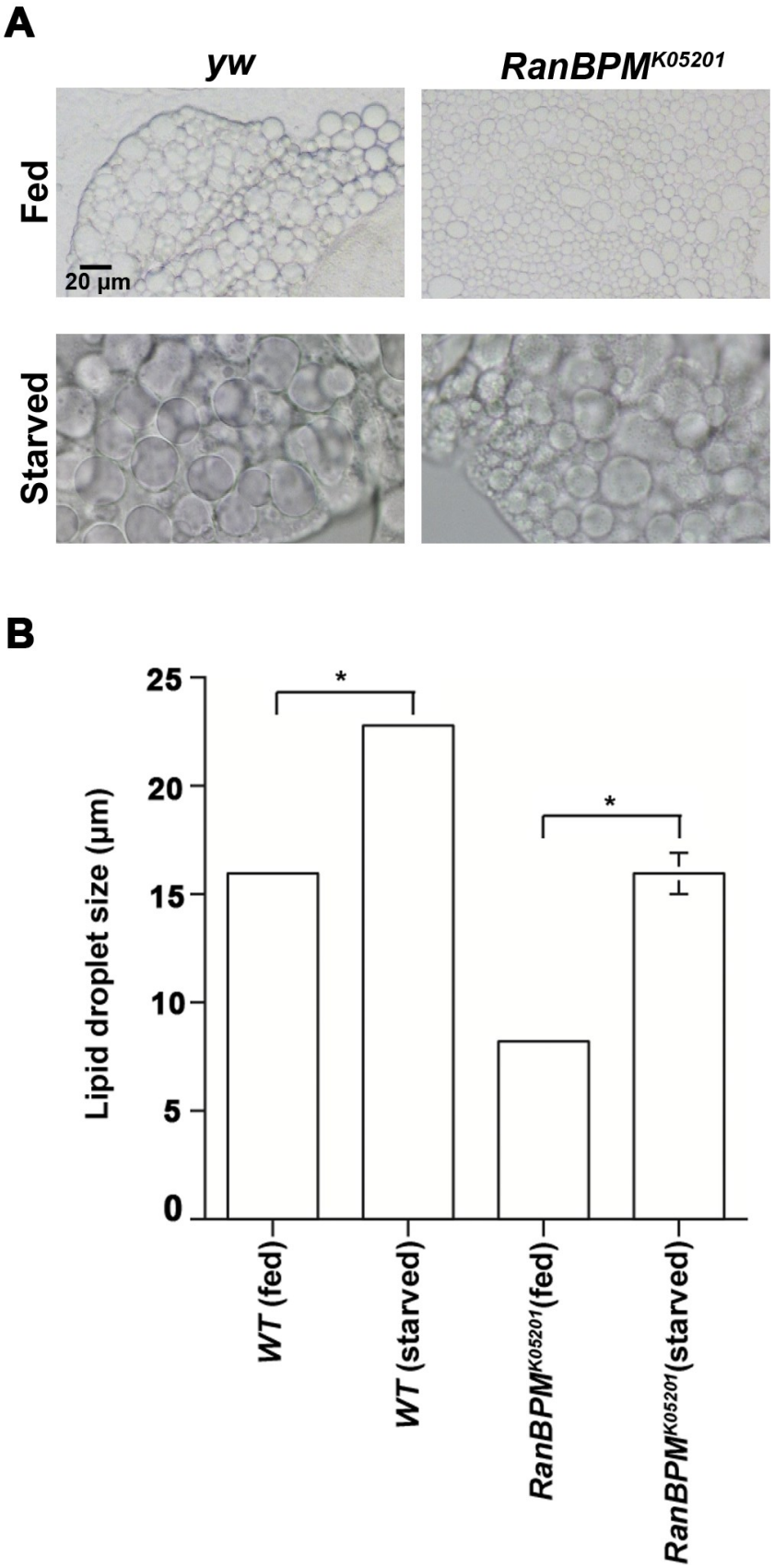
A
yw
RanBPMK05201
Fed
Starved
20 µm
B
Lipid droplet size (µm)
25
20
15
10
5
0
*
*
WT (fed)
WT (starved)
RanBPMK05201(fed)
RanBPMK05201(starved)

Figure 15. Measuring the size of lipid droplets in *RanBPM*^{K05201} mutants under fed and nutrient deprived conditions. Representative micrographs of unstained larval fat body reveal differences in the lipid droplet size as a result of changes in nutritional conditions. Images shown are snapshots taken at bright field setting of **A-** wild type and *RanBPM*^{K05201} mutants under fed conditions as well as wild type and *RanBPM*^{K05201} mutants under starved conditions. The graph depicts the mean diameter of the lipid droplets for the genotypes shown in A. ($N \geq 148$ for each genotype, ANOVA $F(3,1314)=329.32$, $P \leq 0.000$). Mean and SEM values for wild type under fed conditions, wild type after starvation, *RanBPM*^{K05201} mutant under fed and *RanBPM*^{K05201} mutant after starved conditions are 15.950 ± 0.953, 22.774 ± 0.301, 8.197 ± 0.286, 13.821 ± 0.219 respectively.

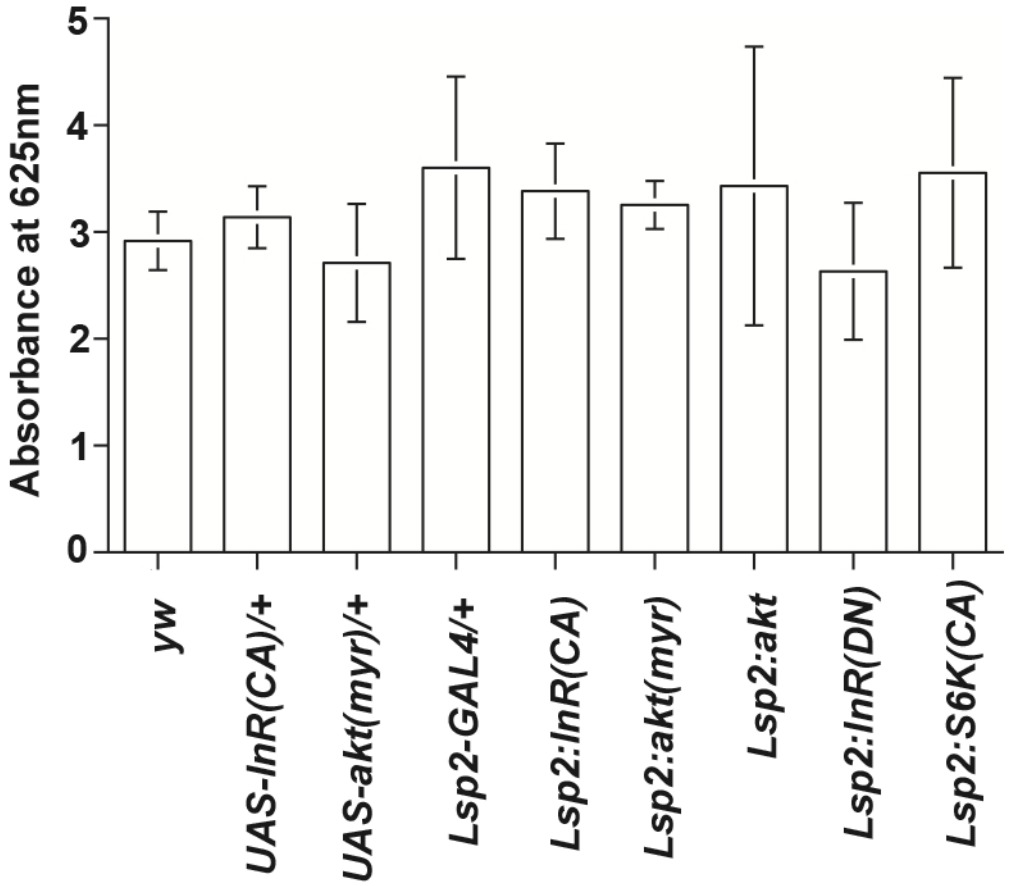

Figure 16. Measure of food intake by modulating insulin signaling in the fat body. The graph depicts the absorbance at 625nm (A665nm) of larval extracts as a measure of the amount of food present in the gut. Various UAS constructs of insulin signaling components were regulated under the control of *Lsp2-GAL4* promoter. *UAS -Akt (myr), UAS-S6k (CA), UAS-Akt, UAS-InR(DN) and UAS-InR(CA)* were expressed under the control of *Lsp2*-GAL4. There was no difference in the A625nm of larval extracts detected in comparison to the appropriate parental controls when these constructs were expressed under the regulation of *Lsp2*-GAL4. All measurements are shown as mean values and +/-

SEM (N ≥2 (60 larvae), ANOVA F(8, 42) = 0.87). No significant difference was found using one way-Anova or two sample T-test analysis.

Additional files

Additional file 1

Indicates homozygous mutant *RanBPM* adult flies in which *RanBPM* expression was restored in the neurosecretory cells under the regulation of *C929-GAL* (*y, w; RanBPM* ^{K05201} *, C929-GAL4/ RanBPM* ^{K05201} *; UAS-RanBPM*). The curly wing flies are heterozygous RanBPM mutants (*y, w; RanBPM* ^{K05201} *, C929-GAL4/ Cy(y+).*

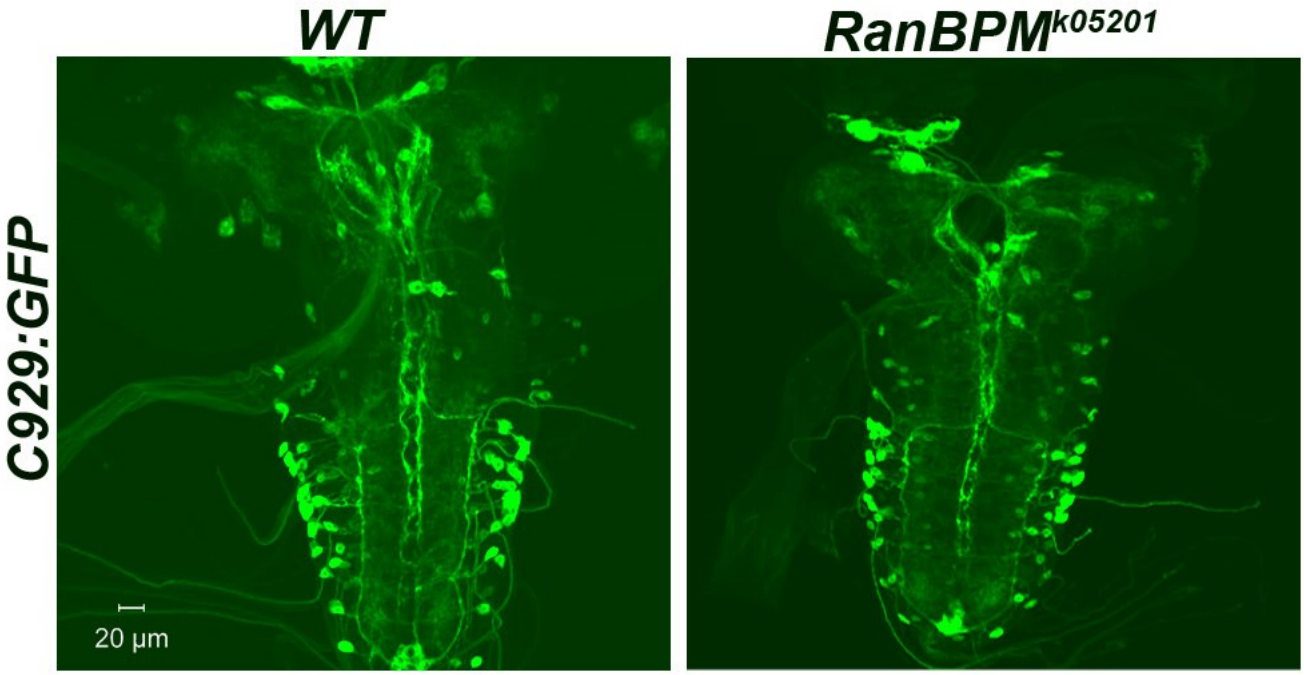

Additional file 2

While the *RanBPM* mutant CNS (right panel) is smaller than wild type controls (left panel) the overall pattern of neurosecretory cell clusters as defined by the expression of GFP under the control of the C929-GAL4 driver is not different from control.

Genotype	mNSC (C929-GAL4 positive)	AKH (AKH-GAL4 positive)	N
WT	15±1.713	8±0.914	20
RanBPM^{k05201}	13±2.038*	8±0.995	22

Additional file 3. Counts of the number of cell in the medial neurosecretory cell (mNSC) clusters located in the pars intercerebralis as identified by the expression of *C929-GAL4*. Adipokinetic hormone (AKH) producing cells located in the ring gland were identified by expression of the *AKH-GAL4* element. In both cases the expression of a nuclear GFP was used to visualize the cells in wild type (WT) or *RanBPM* mutant back ground (*RanBPM*^{K05201}). The number of cells in the mNSC cluster is significantly smaller in *RanBPM* mutants (Student's T test, * p= 0.000).

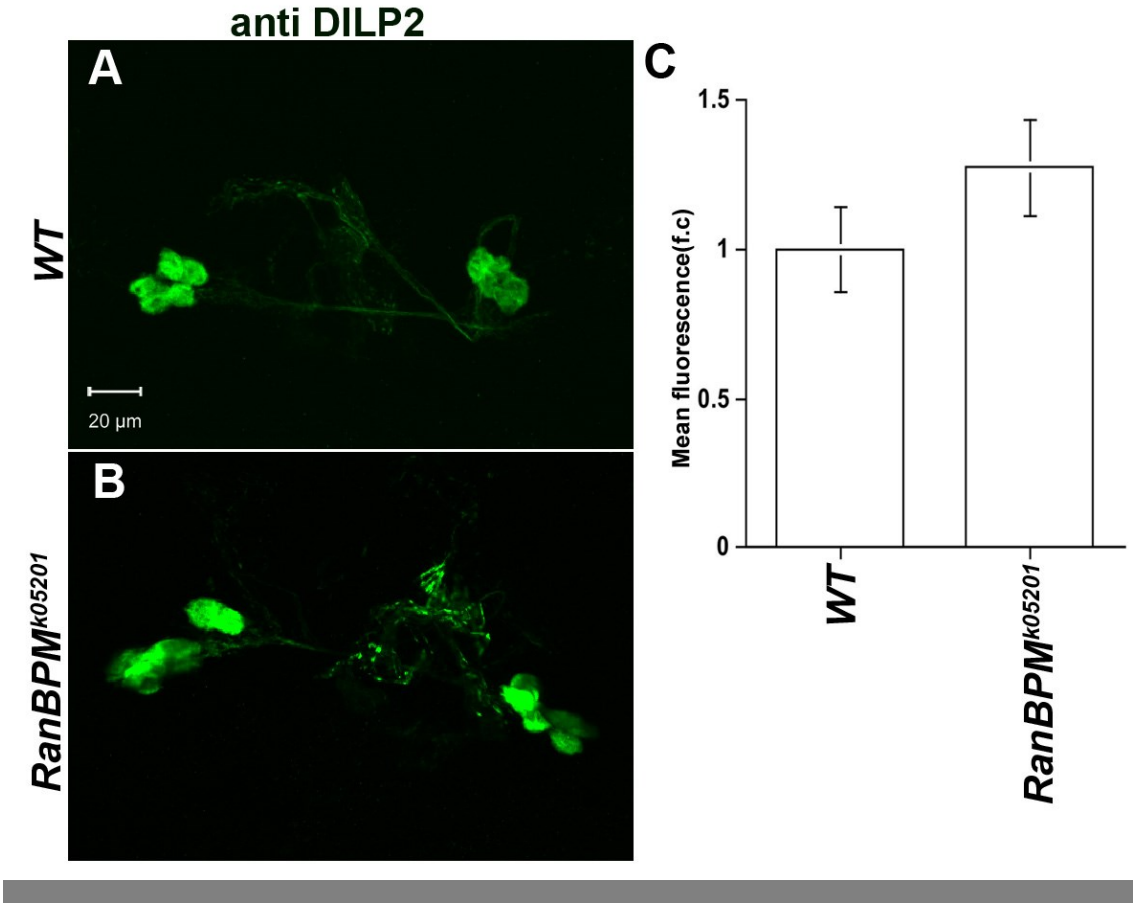

Additional file 4

Second instar *RanBPM* mutant larvae do not display increased accumulation of DILP2 peptide in the insulin producing cells of the brain. Representative photomicrographs of dissected brains from wild type (WT, **A**) or *RanBPM* mutant (*RanBPM*^{K05201}, **B**) second instar larval brains immunolabeled with anti-DILP2 antibodies and imaged by confocal microscopy using the same laser and scan settings. Images represent Z-stacks of 8-12 sections at 1µm intervals. Scale bar in **A** valid for **B.** The graph (**C**) depicts the fluorescence intensity across the insulin producing cell clusters of wild type (WT) and *RanBPM* mutant larvae (*RanBPM*^{K05201}). Fold changes (f.c.) is

indicated relative to the values obtained with the wild type specimens . There is no significant difference between the values measured for both genotypes (N ≥ 30, Student's T test, p= 0.174).

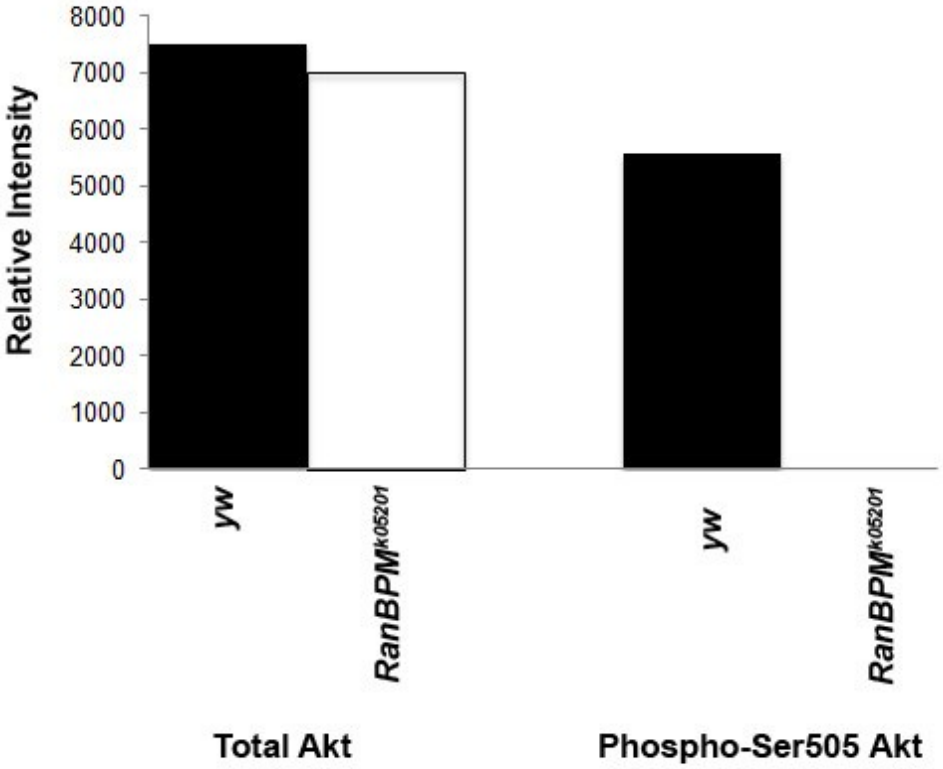

Additional file 5

The graph depicts the relative intensity of the AKT and phospho AKT bands of the western shown in Figure 3C normalized against the actin loading control. The light band detected in the *RanBPM*^{K05201} sample with the antibody that recognizes the phospho active AKT seen in the western is below the level of detection.

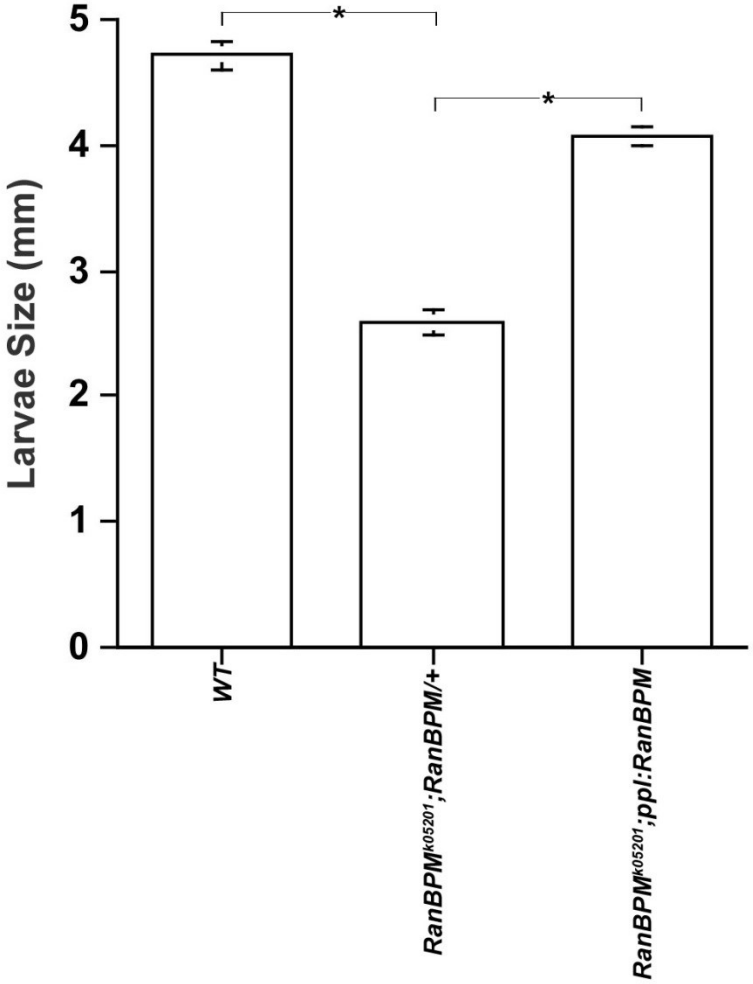

Additional file 6

Targeted expression of *RanBPM* in the fat body under the regulation of *ppl-GAL4* driver partially rescues the size phenotype of *RanBPM* ^{K05201} mutants**.** Image J was used to measure the long axis of larval images. *RanBPM* mutants are significantly smaller than control larvae of the same developmental stage. Restoration of *RanBPM* expression in the fat body of *RanBPM* mutants significantly increased larval size (N $\geq$ 3, ANOVA $F(2,10) = 168{,}22$ $p < 0.01$).

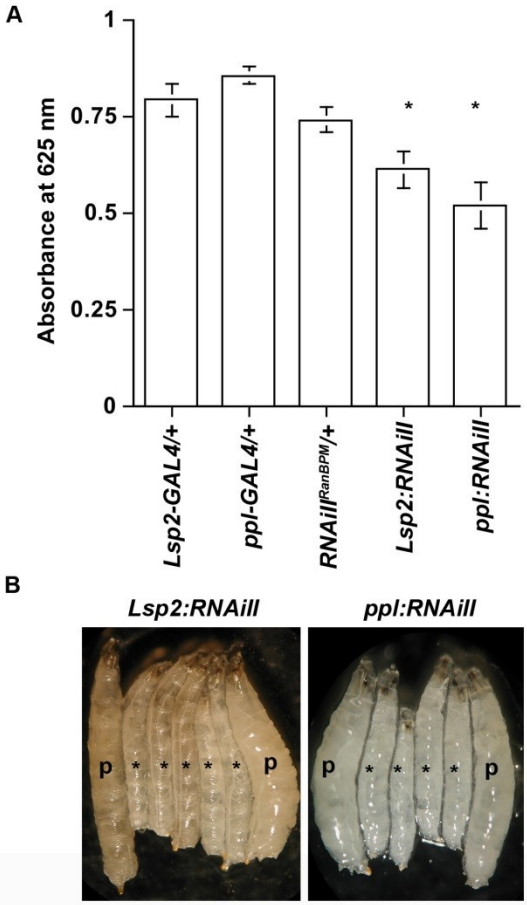

Additional file 7

Fat body RNAi knock down of *RanBPM* gene reduces food accumulation in the gut and disrupts growth. **A**- The graph depicts the absorbance at 625nm (A665nm) of larval extracts as a measure of the amount of food present in the gut. Expression of *dsRNA* construct targeting the *RanBPM* transcript in the fat body using two independent GAL4 drivers significantly reduced the A665nm below that of larvae carrying only one of the GAL4 drivers (*Lsp2-GAL4 or ppl-GAL4*) or the *UAS-RNAII*^{RanBPM} ($N \geq 3$, ANOVA $F(6,27) = 8.15$, $p<0.001$). **B**- Representative micrographs of *Lsp2-RNAII*^{RanBPM} and ppl- *RNAII*^{RanBPM} (*) larvae flanked by parental controls carrying either one of the transgenic constructs.

Literature Cited

Aguila, J.R., Suszko, J., Gibbs, A.G., Hoshizaki, D.K., 2007. The role of larval fat cells in adult Drosophila melanogaster. The Journal of experimental biology 210, 956-963.

Alessi, D.R., James, S.R., Downes, C.P., Holmes, A.B., Gaffney, P.R.J., Reese, C.B., Cohen, P., 1997. Characterization of a 3-phosphoinositide-dependent protein kinase which phosphorylates and activates protein kinase Bα. Current Biology 7, 261-269.

Andersen, D.S., Colombani, J., Leopold, P., 2013. Coordination of organ growth: principles and outstanding questions from the world of insects. Trends Cell Biol.

Arrese, E.L., Soulages, J.L., 2010. Insect fat body: energy, metabolism, and regulation. Annual review of entomology 55, 207-225.

Atabakhsh, E., Wang, J.H., Wang, X., Carter, D.E., Schild-Poulter, C., 2012. RanBPM expression regulates transcriptional pathways involved in development and tumorigenesis. American journal of cancer research 2, 549-565.

Awasaki, T., Ito, K., 2004. Engulfing action of glial cells is required for programmed axon pruning during Drosophila metamorphosis. Current biology : CB 14, 668-677.

Bi, J., Xiang, Y., Chen, H., Liu, Z., Gronke, S., Kuhnlein, R.P., Huang, X., 2012. Opposite and redundant roles of the two Drosophila perilipins in lipid mobilization. Journal of cell science 125, 3568-3577.

Blommaart, E.F., Luiken, J.J., Blommaart, P.J., van Woerkom, G.M., Meijer, A.J., 1995. Phosphorylation of ribosomal protein S6 is inhibitory for autophagy in isolated rat hepatocytes. The Journal of biological chemistry 270, 2320-2326.

Britton, J.S., Edgar, B.A., 1998. Environmental control of the cell cycle in Drosophila: nutrition activates mitotic and endoreplicative cells by distinct mechanisms. Development 125, 2149-2158.

Britton, J.S., Lockwood, W.K., Li, L., Cohen, S.M., Edgar, B.A., 2002. Drosophila's insulin/PI3-kinase pathway coordinates cellular metabolism with nutritional conditions.

Developmental cell 2, 239-249.

Brogiolo, W., Stocker, H., Ikeya, T., Rintelen, F., Fernandez, R., Hafen, E., 2001. An evolutionarily conserved function of the Drosophila insulin receptor and insulin-like peptides in growth control. Current Biology 11, 213-221.

Buch, S., Melcher, C., Bauer, M., Katzenberger, J., Pankratz, M.J., 2008. Opposing effects of dietary protein and sugar regulate a transcriptional target of Drosophila insulin-like peptide signaling. Cell metabolism 7, 321-332.

Butterworth, F.M., Bodenstein, D., King, R.C., 1965. ADIPOSE TISSUE OF DROSOPHILA MELANOGASTER. I. AN EXPERIMENTAL STUDY OF LARVAL FAT BODY. The Journal of experimental zoology 158, 141-153.

Cheng, L., Lemmon, S., Lemmon, V., 2005. RanBPM is an L1-interacting protein that regulates L1-mediated mitogen-activated protein kinase activation. Journal of neurochemistry 94, 1102-1110.

Cheng, L.Y., Bailey, A.P., Leevers, S.J., Ragan, T.J., Driscoll, P.C., Gould, A.P., 2011. Anaplastic lymphoma kinase spares organ growth during nutrient restriction in Drosophila. Cell 146, 435-447.

Colombani, J., Raisin, S., Pantalacci, S., Radimerski, T., Montagne, J., Léopold, P., 2003. A Nutrient Sensor Mechanism Controls Drosophila Growth. Cell 114, 739-749.

Dansereau, D.A., Lasko, P., 2008. RanBPM regulates cell shape, arrangement, and capacity of the female germline stem cell niche in Drosophila melanogaster. The Journal of cell biology 182, 963-977.

Denti, S., Sirri, A., Cheli, A., Rogge, L., Innamorati, G., Putignano, S., Fabbri, M., Pardi, R., Bianchi, E., 2004. RanBPM is a phosphoprotein that associates with the plasma membrane and interacts with the integrin LFA-1. The Journal of biological chemistry 279, 13027-13034.

Garofalo, R.S., 2002. Genetic analysis of insulin signaling in Drosophila. Trends in Endocrinology & Metabolism 13, 156-162.

Geminard, C., Rulifson, E.J., Leopold, P., 2009. Remote control of insulin secretion by fat cells in Drosophila. Cell metabolism 10, 199-207.

Gray, A., Van Der Kaay, J., Downes, C.P., 1999. The pleckstrin homology domains of protein kinase B and GRP1 (general receptor for phosphoinositides-1) are sensitive and selective probes for the cellular detection of phosphatidylinositol 3,4-bisphosphate and/or phosphatidylinositol 3,4,5-trisphosphate in vivo. The Biochemical journal 344 Pt 3, 929-936.

Grewal, S.S., 2009. Insulin/TOR signaling in growth and homeostasis: a view from the fly world. The international journal of biochemistry & cell biology 41, 1006-1010.

Gutierrez, E., Wiggins, D., Fielding, B., Gould, A.P., 2007. Specialized hepatocyte-like cells regulate Drosophila lipid metabolism. Nature 445, 275-280.

Hassan, J., Iyengar, B., Scantlebury, N., Rodriguez Moncalvo, V., Campos, A.R., 2005. Photic input pathways that mediate the Drosophila larval response to light and circadian rhythmicity are developmentally related but functionally distinct. The Journal of comparative neurology 481, 266-275.

Hyun, S., 2013. Body size regulation and insulin-like growth factor signaling. Cellular and molecular life sciences : CMLS.

Iijima, K., Zhao, L., Shenton, C., Iijima-Ando, K., 2009. Regulation of energy stores and feeding by neuronal and peripheral CREB activity in Drosophila. PLoS One 4, e8498.

Ikeya, T., Galic, M., Belawat, P., Nairz, K., Hafen, E., 2002. Nutrient-Dependent Expression of Insulin-like Peptides from Neuroendocrine Cells in the CNS Contributes to Growth Regulation in Drosophila. Current Biology 12, 1293-1300.

Juhasz, G., Neufeld, T., 2008. Experimental Control and Characterization of Autophagy in Drosophila, in: Deretic, V. (Ed.), Autophagosome and Phagosome. Humana Press, pp. 125-133.

Lazareva, A.A., Roman, G., Mattox, W., Hardin, P.E., Dauwalder, B., 2007. A role for the

adult fat body in Drosophila male courtship behavior. PLoS genetics 3, e16.

Lemaitre, B., Hoffmann, J., 2007. The host defense of Drosophila melanogaster. Annual review of immunology 25, 697-743.

McBride, S.M., Bell, A.J., Jongens, T.A., 2012. Behavior in a Drosophila model of fragile X. Results and problems in cell differentiation 54, 83-117.

Murrin, L.C., Talbot, J.N., 2007. RanBPM, a scaffolding protein in the immune and nervous systems. Journal of neuroimmune pharmacology : the official journal of the Society on
NeuroImmune Pharmacology 2, 290-295.

Nishitani, H., Hirose, E., Uchimura, Y., Nakamura, M., Umeda, M., Nishii, K., Mori, N., Nishimoto, T., 2001. Full-sized RanBPM cDNA encodes a protein possessing a long stretch of proline and glutamine within the N-terminal region, comprising a large protein complex. Gene 272, 25-33.

Oldham, S., Hafen, E., 2003. Insulin/IGF and target of rapamycin signaling: a TOR de force in growth control. Trends in Cell Biology 13, 79-85.

Park, D., Taghert, P.H., 2009. Peptidergic neurosecretory cells in insects: organization and control by the bHLH protein DIMMED. General and comparative endocrinology 162, 2-7.

Park, D., Veenstra, J.A., Park, J.H., Taghert, P.H., 2008. Mapping Peptidergic Cells in *Drosophila*: Where DIMM Fits In. PLoS ONE 3, e1896.

Petiot, A., Ogier-Denis, E., Blommaart, E.F., Meijer, A.J., Codogno, P., 2000. Distinct classes of phosphatidylinositol 3'-kinases are involved in signaling pathways that control macroautophagy in HT-29 cells. The Journal of biological chemistry 275, 992-998.

Rajan, A., Perrimon, N., 2011. Drosophila as a model for interorgan communication: lessons from studies on energy homeostasis. Developmental cell 21, 29-31.

Rameh, L.E., Cantley, L.C., 1999. The Role of Phosphoinositide 3-Kinase Lipid Products in

Cell Function. Journal of Biological Chemistry 274, 8347-8350.

Raught, B., Gingras, A.C., Sonenberg, N., 2001. The target of rapamycin (TOR) proteins. Proceedings of the National Academy of Sciences of the United States of America 98, 7037-7044.

Reiling, J.H., Hafen, E., 2004. The hypoxia-induced paralogs Scylla and Charybdis inhibit growth by down-regulating S6K activity upstream of TSC in Drosophila. Genes & development 18, 2879-2892.

Rodriguez Moncalvo, V.G., Campos, A.R., 2009. Role of serotonergic neurons in the Drosophila larval response to light. BMC neuroscience 10, 66.

Scantlebury, N., Zhao, X.L., Rodriguez Moncalvo, V.G., Camiletti, A., Zahanova, S., Dineen, A., Xin, J.H., Campos, A.R., 2010. The Drosophila gene RanBPM functions in the mushroom body to regulate larval behavior. PLoS One 5, e10652.

Scott, R.C., Schuldiner, O., Neufeld, T.P., 2004. Role and regulation of starvation-induced autophagy in the Drosophila fat body. Developmental cell 7, 167-178.

Sepp, K.J., Schulte, J., Auld, V.J., 2001. Peripheral glia direct axon guidance across the CNS/PNS transition zone. Developmental biology 238, 47-63.

Sousa-Nunes, R., Cheng, L.Y., Gould, A.P., 2010. Regulating neural proliferation in the Drosophila CNS. Current opinion in neurobiology 20, 50-57.

Sousa-Nunes, R., Yee, L.L., Gould, A.P., 2011. Fat cells reactivate quiescent neuroblasts via TOR and glial insulin relays in Drosophila. Nature 471, 508-512.

Teleman, A.A., 2010. Molecular mechanisms of metabolic regulation by insulin in Drosophila. The Biochemical journal 425, 13-26.

Ullrich, A., Schlessinger, J., 1990. Signal transduction by receptors with tyrosine kinase activity. Cell 61, 203-212.

Verdu, J., Buratovich, M.A., Wilder, E.L., Birnbaum, M.J., 1999. Cell-autonomous

regulation of cell and organ growth in Drosophila by Akt/PKB. Nat Cell Biol 1, 500-506.

Wang, D., Li, Z., Messing, E.M., Wu, G., 2002. Activation of Ras/Erk pathway by a novel MET-interacting protein RanBPM. The Journal of biological chemistry 277, 36216-36222.
Yang, S.N., Berggren, P.O., 2006. The role of voltage-gated calcium channels in pancreatic beta-cell physiology and pathophysiology. Endocrine reviews 27, 621-676.

Yin, Y.X., Sun, Z.P., Huang, S.H., Zhao, L., Geng, Z., Chen, Z.Y., 2010. RanBPM contributes to TrkB signaling and regulates brain-derived neurotrophic factor-induced neuronal morphogenesis and survival. Journal of neurochemistry 114, 110-121.

Yokoyama, N., Hayashi, N., Seki, T., Pante, N., Ohba, T., Nishii, K., Kuma, K., Hayashida, T., Miyata, T., Aebi, U., et al., 1995. A giant nucleopore protein that binds Ran/TC4. Nature 376, 184-188.

Yuan, Y., Fu, C., Chen, H., Wang, X., Deng, W., Huang, B.R., 2006. The Ran binding protein RanBPM interacts with TrkA receptor. Neuroscience letters 407, 26-31.

Zhang, H., Stallock, J.P., Ng, J.C., Reinhard, C., Neufeld, T.P., 2000. Regulation of cellular growth by the Drosophila target of rapamycin dTOR. Genes & development 14, 2712-2724.

Zhao, X.L., Campos, A.R., 2012. Insulin signalling in mushroom body neurons regulates feeding behaviour in Drosophila larvae. The Journal of experimental biology 215, 2696-2702.

Zinke, I., Kirchner, C., Chao, L.C., Tetzlaff, M.T., Pankratz, M.J., 1999. Suppression of food intake and growth by amino acids in Drosophila: the role of pumpless, a fat body expressed gene with homology to vertebrate glycine cleavage system. Development 126, 5275-5284.